Adamson R, Hobbs M, Silcock A, Willis MJ.

Integrated real-time production scheduling of a multiple cryogenic air separation unit and compressor plant.

***Computers and Chemical Engineering* 2017, 104, 25-37.**

Integrated real-time production scheduling of a multiple cryogenic air separation unit and compressor plant

Richard Adamson[a], Martin Hobbs[b], Andy Silcock[b] and Mark J. Willis[a]
[a]School of Chemical Engineering and Advanced Materials, Newcastle University, Newcastle upon Tyne, NE1 7RU, United Kingdom
[b]BOC Gases Ltd., Bawtry Road, Brinsworth, Rotherham, S60 5NT, United Kingdom
richard.adamson1@newcastle.ac.uk, mark.willis@newcastle.ac.uk

Abstract

The development and application of an integrated real-time production scheduling and control strategy for a multiple cryogenic air separation unit (ASU) and compressor plant is discussed. Using a top-down optimisation approach, the operational targets for ASU production and compressor configuration are obtained for a given customer demand and subsequently managed using a real-time optimisation strategy. This is integrated with existing control to implement the steady-state configuration targets subject to process disturbances, power price fluctuations and against network change penalty weightings. Network material balance and network component operating constraints are met while simultaneously minimising plant reconfiguration costs during transient operation which occurs as a result of changing demands. Implemented using mixed integer linear programming, it is demonstrated that the two-stage optimisation strategy improves site operating costs by an average of 5% over the considered trial period (which would translate into substantial cost savings for such an energy intensive process).

Keywords: production scheduling, site-wide optimisation, real-time optimisation, control, power consumption, mixed integer linear programming.

Highlights

- Application of production scheduling with real-time optimisation.
- Integration of site-wide and real-time optimisation with existing MPC strategies.
- Management of ASU transitions and compression network change within RTO.
- Optimisation implemented using mixed integer linear programming.

Nomenclature

Abbreviations

ASU	– air separation unit	GO	– gaseous oxygen
HCM	– hundred cubic meters	HP	– high pressure
IC	– internally compressed	LN	– liquid nitrogen
LO	– liquid oxygen	LP	– low pressure
MPC	– model based predictive control	ME	– model mean error (kW)
MP	– medium pressure	RTO	– real-time optimisation
SSO	– steady-state optimisation	SWO	– site-wide optimisation
TGO	– total gaseous oxygen demand	TLO	– total liquid oxygen

Parameters

$\hat{b}$	– model co-efficient	β	– max ramp rate (m^3/hr^2)
C_{kW}	– spot power cost (£/MWh)	C_{LO}	– liquid make cost (£/m^3)
C_s	– liquid use cost (£/m^3)	g	– compressor on penalty (£)

h	– compressor off penalty (£)	J	– cost function (£/hr)
P_{Dj}	– discharge pressure (bar)	W	– power consumption (kW)
$\widehat{W}$	– power consumption estimation (kW)	μ	– average
τ	– compression change penalty (£)	ρ	– control error penalty (£)
σ	– ASU change penalty (£)	φ	– LP spill penalty (£)
Variables			
δ	– binary co-efficient	F	– flow rate (m^3/hr)
y	– total flow/binary auxiliary variable	z	– penalty auxiliary variable
Subscript/Superscripts			
c	– compressor	j	– compressor or ASU number
k	– pseudo-machine number	m	– model number
max	– maximum capacity limit	min	– minimum capacity limit
$RAMP$	– ramping customer demand	REQ	– requested customer demand
s	– liquid back-up supply	SW	– site-wide
t	– discrete time point	u	– unit (ASU)
v	– valve	RT	– real-time

1.0 Introduction

Cryogenic air separation is a highly energy intensive process[1], with optimal operation critical to minimise energy consumption of sites; which often consist of an elaborate network of air separation units (ASUs) and compressors. This is particularly important where external market conditions, such as customer demand and power pricing, change, as the entire plant must be reconfigured to trade-off power consumption with specific demand requirements. In the literature, there are many examples of network optimisation by load and production sharing, see reviews by Cortinovis et al. (2016) and Xenos et al. (2015), where load sharing control can be effectively achieved after integration with existing control schemes.

However, only a few published papers have considered implementing a real-time optimisation (RTO) approach to manage the optimal load sharing of a network of compressors (and ASUs) and the subsequent integration with process control schemes. Cortinovis et al. (2016) note that only Xenos et al. (2015) and Paperella et al. (2014) have come close to the implementation of RTO; with Xenos et al. (2015) investigating the optimisation of cryogenic air separation networks (along with maintenance scheduling) using a mixed integer nonlinear programming (MINLP) network model and Paparella et al. (2014) examining RTO of natural gas compression station networks. Cortinovis et al. (2016) themselves develop a load sharing strategy based on the simulation of a large compression plant implemented as a MINLP problem but with high solving times. They also highlight requirement for the development of a computationally efficient method to consider network reconfiguration costs, such as the abortive power costs of changing product compression.

In other examples, Puranik et al. (2016) optimise an air separation plant configuration to meet changing demand requirements, where operating cost minimisation is the primary goal. They argue uncertainty in electricity price forecasts (perhaps due to increased uncertainty in renewable generation, demand and power market conditions) and unpredictable gas pipeline customer demands favour the use of RTO over discrete time optimal scheduling of future

[1] e.g. the Air Liquide Group's total electricity consumption in 2010 corresponded to more than one thousandth of the world's total electricity consumption, Li et al. (2011), and the industrial gas industry used approximately 3.5% of the total industrial electricity consumption of the US in 1998, Zhou et al. (2017).

activities. Zhu et al. (2011) discuss optimisation of air separation plants with forecasts of variable power pricing. In addition, Zhou et al. (2017) discuss current limitations in the literature where works typically only focus on the scheduling of individual ASUs. The consideration of multiple ASUs that flex and load share over time to meet changing customer gas demands provides a more industrially relevant and challenging problem. Therefore, the novel site-wide steady-state optimisation (SSO) deployed in Adamson et al. (2017) requires extension into a robust RTO strategy to ensure optimal network management at all times, i.e. during demand changes and accounting for process disturbances such as variable power pricing and pipeline pressures.

The cooperation of site-wide optimisation (SWO) and the lower level control systems is an important field of research which has practical significance. The importance of the current work is highlighted by a recent funding call, European Commission (2015), noting the current shortcomings in integration of dedicated local control systems with overarching real-time optimisation scheduling systems for the control and monitoring of processes. The review by Baldea and Harjunkoski (2014) proposes the fact that the scheduling and control fields evolved separately, along with current inefficiencies in communication and solving strategies, as the reason for why efforts to integrate these strategies have only recently begun. Lotero (2017) suggest the scheduling community focussed on online scheduling and the control community only considered closed loop implementations, with the methods not converging. Combined RTO and control strategies must simultaneously consider production, operational and control law constraints as well as defining the overall objective function goal. Recent works to integrate the strategies include, Marchetti et al. (2014), Tatjewski (2010) and Hovd (2007) whom all suggest the use of an end-point target optimiser to generate set point optimisation goals and an additional (normally linear) RTO layer to minimise actual to target set point errors. Marchetti et al. (2014) describe how the outputs of SSO can be used a target for other layers of control to achieve optimal economic operation. In their work, they note that in the face of the disturbances the SSO may not correspond to a currently feasible operation therefore a further RTO layer is required prior to implementation via model based predictive control (MPC). Tatjewsji (2010) describes a method to model uncertainty in the RTO layer enabling economic optimisation subject to modelled process constraints. Finally, Hovd (2007) note that RTO can be used to find a feasible operating point close to the SSO target using current disturbance data therefore reducing model errors caused by process uncertainties changing the optimal operating point. One example of the application of multilayer control with SSO targets is Singh et al. (2015) who adopt an integrated moving horizon based approach to optimise a continuous compaction tablet manufacturing process.

This paper reports the successful development and application of a novel RTO strategy to a real multiple cryogenic ASU and compressor plant demonstrating optimal load and production sharing in conjunction with optimal reconfiguration timing, implemented to achieve a significant financial benefit. Our RTO strategy is like the economic MPC approaches of Würth et al. (2009), Engell (2009) and Heidarinejad et al. (2012), where the tracking objective function of standard MPC is replaced by an economics based (usually nonlinear) objective function. However, as opposed to integrating this with MPC, this is used at steady-state (with steady-state models) to co-ordinate the load sharing optimisation problem, i.e. co-ordinate the set points transmitted to the individual MPCs, efficiently.

Work detailed in Pattison et al. (2016), describes the need for scheduling and MPC control strategies which operate at different frequencies to react to economic information changing at dissimilar rates. They suggest the need for detailed dynamics to be included in an RTO strategy, with scale-bridging models used to tie the optimisation and control layers for real-time solvability. However, this is at variance with our work as there was no possibility of

investigating modifications to the well-established MPC proprietary software; so the layers had to remain separate and further work is required to challenge our assumption that unmodelled dynamics affect model robustness. Furthermore, as our results demonstrate, dynamics are not required to be captured in the RTO layer as a) the model based and supervisory control schemes already in place can control high frequency dynamic disturbances to ensure stable plant operation and b) the RTO strategy tracks the output of the scheduling layer following a contractually agreed ramping policy.

We develop a computationally efficient mixed integer linear programming (MILP) approach to RTO designed to cooperate with the process plant control system to achieve optimal plant operation and reconfiguration timing. Using a piece-wise linear modelling strategy and solving the resulting optimisation problem using MILP, our previously developed site-wide SSO strategy successfully discovers the optimal network configuration for any demand request. However, it is not adequate during periods where the network configuration is being altered to meet these changing demands or able to cope in the face of process disturbances. This is because contractual policy dictates that optimal ASU set points must be achieved via a contractual 'ramping policy'. Therefore, to develop a robust implementation in this paper we propose to use the site-wide steady-state optimiser as a target set point optimiser and develop a second, RTO strategy. This is used to determine the optimal transition from the current network ASU production distribution and compression configuration to the target optimal, subject to meeting the contractual changing customer demand at all times and adhering to safe operational constraints such as maximum ASU ramp rates. Network reconfiguration is carried out by periodically manipulating the ASU production flow rate set points and optimally timing the compression selection changes to meet customer demands and reduce losses. Both the SWO and RTO strategies are required to generate set targets for the underlying control schemes immediately in order to meet contractual changes in customer demand, which begin on order change.

The developed control and scheduling framework solves inside an automated and accessible Microsoft Excel spreadsheet environment for ease of use and integration with existing control strategies. The optimisers operate the Solver add-in simplex linear programming algorithm which automatically deploys the branch and bound method to return the globally optimal solution to the MILP SWO problem within seconds for RTO of network transitions to begin immediately on demand change, following the customer gas supply contract requirements. Large solving times in the SWO layer caused by complex nonlinear modelling techniques were therefore not an option to be integrated within a spreadsheet optimisation environment.

The two stage optimisation strategy demonstrates considerable operational and financial benefits including reduction of power consumption during network transitions, minimisation of liquid back up consumption, reduction of low pressure gaseous oxygen spill and the costs and optimal timing of switching compressors – something that, to the authors best knowledge, has not been considered in the literature. SWO produces stable scheduled optimal targets for a given combination of demands using fixed power pricing and operational data to which the RTO strategy must navigate, subject to changes in power pricing, process conditions and meeting the ramping demand. The RTO solves an optimal control problem; penalising excessive network configuration changes (turning on or off compressors) to obtain the optimal solution for the given point in the network transition. Furthermore, the proposed method allows the consideration of periodically fluctuating power pricing and its effect on flexible loads such as product compression (as ASU power is purchased on a different market and only flexed to meet customer demand changes), changing machine availability (due to maintenance or unexpected break-down) and process variables to enable realistic modelling and cost optimisation, even during network transitions.

1.1 The multiple cryogenic air separation unit and compressor plant

The multiple cryogenic air separation unit (ASU) and compressor plant considered in this work is a gaseous oxygen (GO) supply network operated to meet customer flow demands, in the scale of hundred cubic meters per hour, at two pressures, medium pressure (MP) at 15 bar and high pressure (HP), which is highly variable up to 40 bar. A schematic of the network is shown in Figure 1 with the network flow component descriptions in Table 1. It comprises a complex network of product gas compressors fed by three ASUs which provide production flows of gaseous and liquid oxygen from compressed air feeds. GO is compressed and sent directly to the customer while liquid oxygen (LO) is stored in vessels on site for gas network back up during compressor trips, to meet customer demands at times of high electricity prices and to meet local bulk liquid customer demands by road tanker. Two ASUs produce low pressure (LP) and the third is an internally compressed (IC) ASU capable of producing MP and HP GO directly, along with liquid nitrogen (LN).

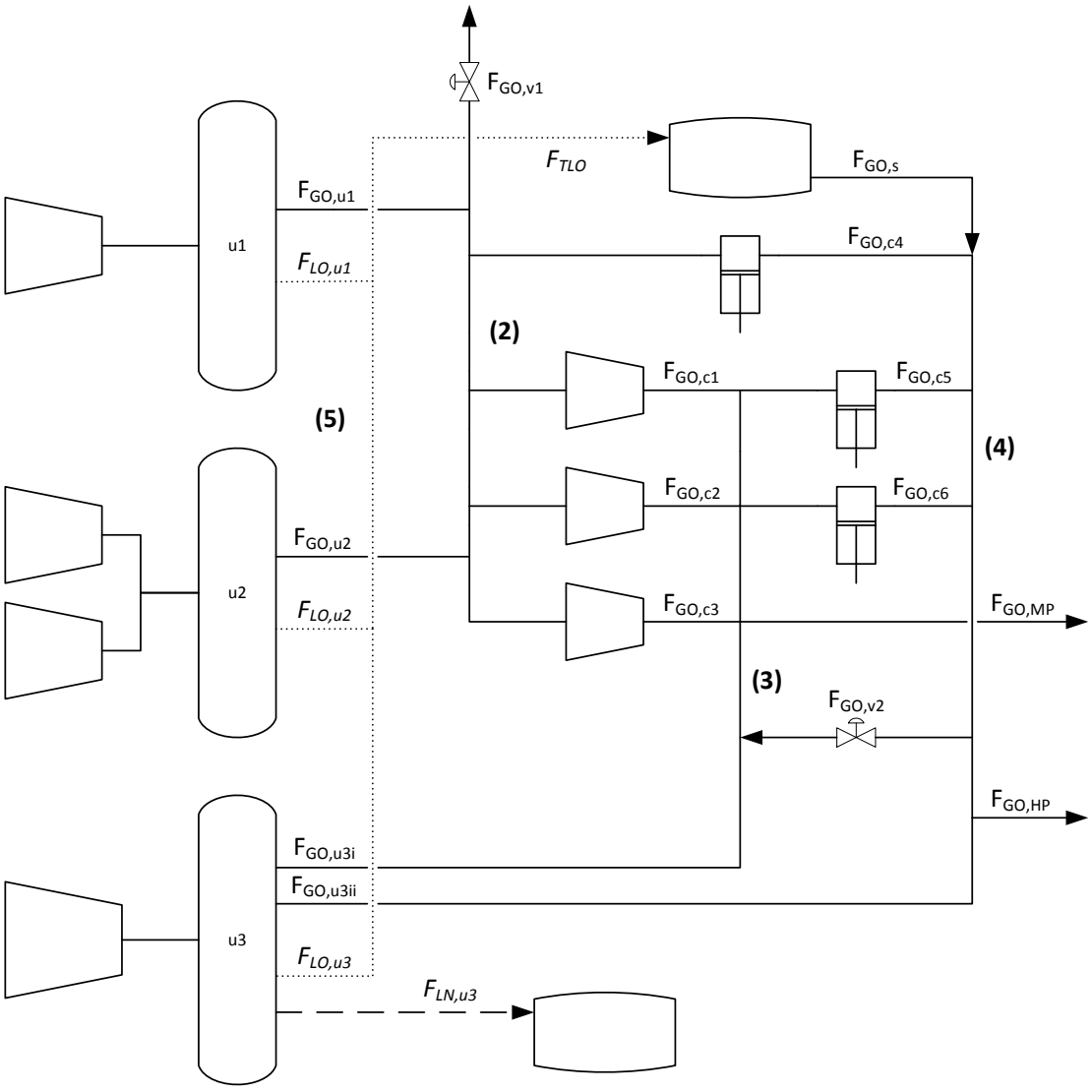

Figure 1: Margam supply network and compression configuration for oxygen production (Table 1 provides a description of each network flow) reproduced from Adamson et al. (2017). The network comprises of three air separation units (ASUs) (u1, u2 and u3) fed by four air compressors, three centrifugal oxygen compressors (c1, c2 and c3), three reciprocating oxygen compressors (c4, c5 and c6), one spill valve (v1), one cross-over valve (v2), back up liquid oxygen vaporisation supply ($F_{GO,s}$) and flows of liquid oxygen (F_{LO}) and liquid nitrogen (F_{LN}) to storage tanks. Highlighted points (numbers) correspond to the equation number of developed mass balances, shown by the equations (2) – (5).

Table 1: Margam oxygen gas supply and compression network flow components and descriptions.

Flow	Description
$F_{GO,u1}$	Production flow of gaseous LP oxygen from ASU u1
$F_{GO,u2}$	Production flow of gaseous LP oxygen from ASU u2
$F_{GO,u3i}$	Production flow of gaseous MP oxygen from ASU u3
$F_{GO,u3ii}$	Production flow of gaseous HP oxygen from ASU u3
$F_{GO,c1}$	LP to MP oxygen flow through centrifugal compressor c1
$F_{GO,c2}$	LP to MP oxygen flow through centrifugal compressor c2
$F_{GO,c3}$	LP to MP oxygen flow through centrifugal compressor c3
$F_{GO,c4}$	LP to HP oxygen flow through reciprocating compressor c4
$F_{GO,c5}$	MP to HP oxygen flow through reciprocating compressor c5
$F_{GO,c6}$	MP to HP oxygen flow through reciprocating compressor c6
$F_{GO,v1}$	Flow of oxygen spilled from the LP line through valve v1
$F_{GO,v2}$	Flow of oxygen expanded from HP to MP through valve v2
$F_{GO,s}$	Flow of oxygen vaporised from liquid oxygen storage
$F_{GO,MP}$	Flow of MP oxygen to the customer
$F_{GO,HP}$	Flow of HP oxygen to the customer
$F_{LO,u1}$	Production flow of liquid oxygen from ASU u1
$F_{LO,u2}$	Production flow of liquid oxygen from ASU u2
$F_{LO,u3}$	Production flow of liquid oxygen from ASU u3
F_{TLO}	Total production flow of liquid oxygen from all ASUs to storage
$F_{LN,u3}$	Production flow of liquid nitrogen from ASU u3

1.2 Current operating policy

Figure 2 shows the current network operational procedure and control scheme. Demand combinations of MP GO ($F_{GO,MP\ REQ}$) and HP GO ($F_{GO,HP\ REQ}$) are conveyed to the site shift manager by the customer over the telephone when an order change is required. Often, to meet the new demand order, ASU production rate set points and the compression network configuration must be manipulated from the current arrangement using the MPC schemes. The MPC schemes ensure ASU internal material and energy balances are met, maintaining safe control, product purity and production flow rates at all times, as described in Schmidt et al. (2001). The effect of process disturbances, such as unexpected purity changes and valve actuator failures are neutralised by the MPC laws and local PI(D) control layers which ramp air compressors to meet the required GO set point targets. However, the ASU production rate set point targets are still required to be periodically input by the shift operators, following site operational logic, and compressors brought in and out of service manually, with the decision making process and configuration change timing often being non-optimal.

Shift operators attempt to minimise the overall power usage, LP GO spill and LO back up supply losses of the plant at all times during the process transition but this is a difficult task as all network components vary in specifications, including capacities and efficiencies and the operator must plan network manipulation in advance without scheduling tools. Some current reconfiguration strategies include ramping ASU production rates individually in order to meet changes in customer demand instead of optimally load sharing between units and inefficiently loading compressors rather than changing the current configuration by swapping machines in service. Further, the timing of transitions is critical to minimise network losses as removing compressors from service early may lead to customer undersupply, resulting in liquid oxygen consumption from back up and gaseous spill.

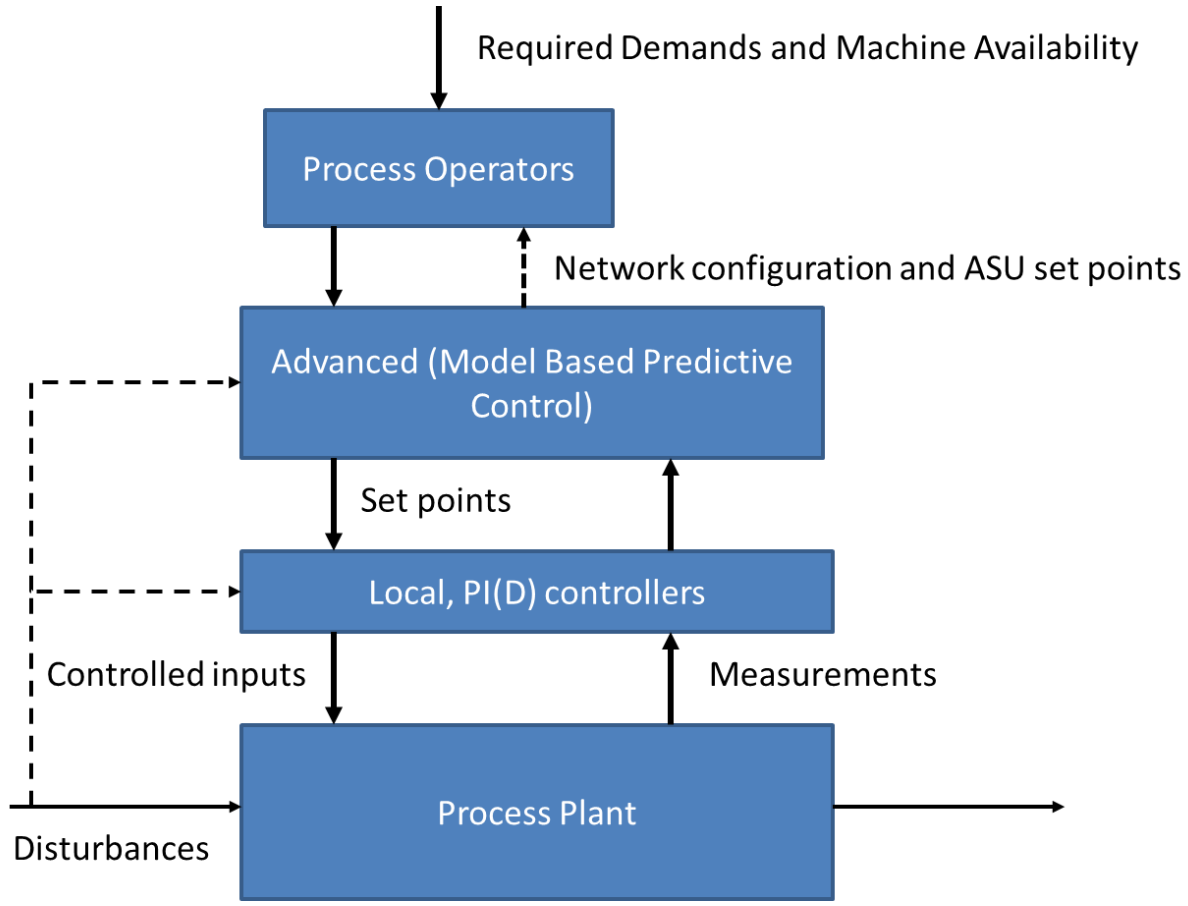

Figure 2: Current network operation control schemes and operational procedure showing operator interaction with the control system hierarchy. Whilst advanced MPBC is used to maintain ASU internal material and energy balances, safe control, product purity and production flow rates at all times, the ASU production rate set point targets are periodically input by the shift operators, following site operational logic, and compressors brought in and out of service manually. Due to reliance on the process operators, sub-optimal load sharing and reconfiguration timing can result, hence increased operating costs.

1.3 Ramping customer demands

Throughout the transition between customer demands, process operators must ensure the metered MP GO, $F_{GO,MP}$, and HP GO, $F_{GO,HP}$, flows meet contractual 'ramping demand' targets, $F_{GO,MP\ RAMP,t}$ and $F_{GO,HP\ RAMP,t}$ by manipulating ASU production rate set points and bringing compressors in and out of service in a timely manner. Ramping demands are implemented as new customer demands cannot be supplied immediately due to required network reconfiguration strategies and safe hourly ASU ramping limits, $\left(\frac{dF_{GO,uj}}{dt}\right)_{max}$, ($m^3/hr^2$) which are enforced by plant managers to prevent major ASU plant upset.

The feasible pipeline flow ramp demand changes, $\frac{dF_{GO,MP}}{dt}$ and $\frac{dF_{GO,HP}}{dt}$, (m^3/hr^2) will depend on the number of ASUs running, the individual agreed safe ASU production flow ramp rates, (which may be different for each ASU) and what has changed since the last requested demand. For example, suppose that the current number of ASUs running is three then the maximum ramp rates are given by (where $\beta\ dt$ is a constant maximum ramp rate divided by the ramping demand calculation frequency),

$$\frac{dF_{GO,MP}}{dt} + \frac{dF_{GO,HP}}{dt} = \sum_{j=1}^{3}\left(\frac{dF_{GO,uj}}{dt}\right)_{max} = \beta\ dt \qquad (1)$$

The contract with the customer agrees that if a change in only MP or HP is requested, the entire available ramp can be allocated to that changing pressure GO flow. If both the MP and HP request has changed, half the available ramp rate is allocated to each supplied pressure. If there is a demand increase in one gas pressure and a decrease in another then overall there is no production change and the full available ramp change is allocated to each pressure.

The available ramp rate, calculated by equation 1, is either added or subtracted to the current value of the ramped demand (depending on whether the ramp is increasing or decreasing the production requirement). For example, to calculate an increase in the ramping MP demand, where $F_{GO,MP\ RAMP} < F_{GO,MP\ REQ}$ then,

$$F_{GO,MP\ RAMP,t} = F_{GO,MP\ RAMP,t-1} + \beta\ dt$$

Whereas, if both the MP and HP request has changed and, for example, $F_{GO,MP\ RAMP,t} < F_{GO,MP\ REQ}$ and $F_{GO,HP\ RAMP,t} < F_{GO,HP\ REQ}$ then,

$$F_{GO,MP\ RAMP,t} = F_{GO,MP\ RAMP,t-1} + \frac{\beta}{2}dt,$$

$$F_{GO,HP\ RAMP,t} = F_{GO,HP\ RAMP,t-1} + \frac{\beta}{2}dt$$

This ramping ends when the requested demands equal the metered supply i.e. $F_{GO,MP\ RAMP,t} = F_{GO,MP\ REQ}$ and $F_{GO,HP\ RAMP,t} = F_{GO,HP\ REQ}$. Figure 3 shows a typical period of three days customer requested demand of MP and HP GO and the sum, total gaseous oxygen (TGO) demand. The contractual ramping demands are calculated and shown on the figure.

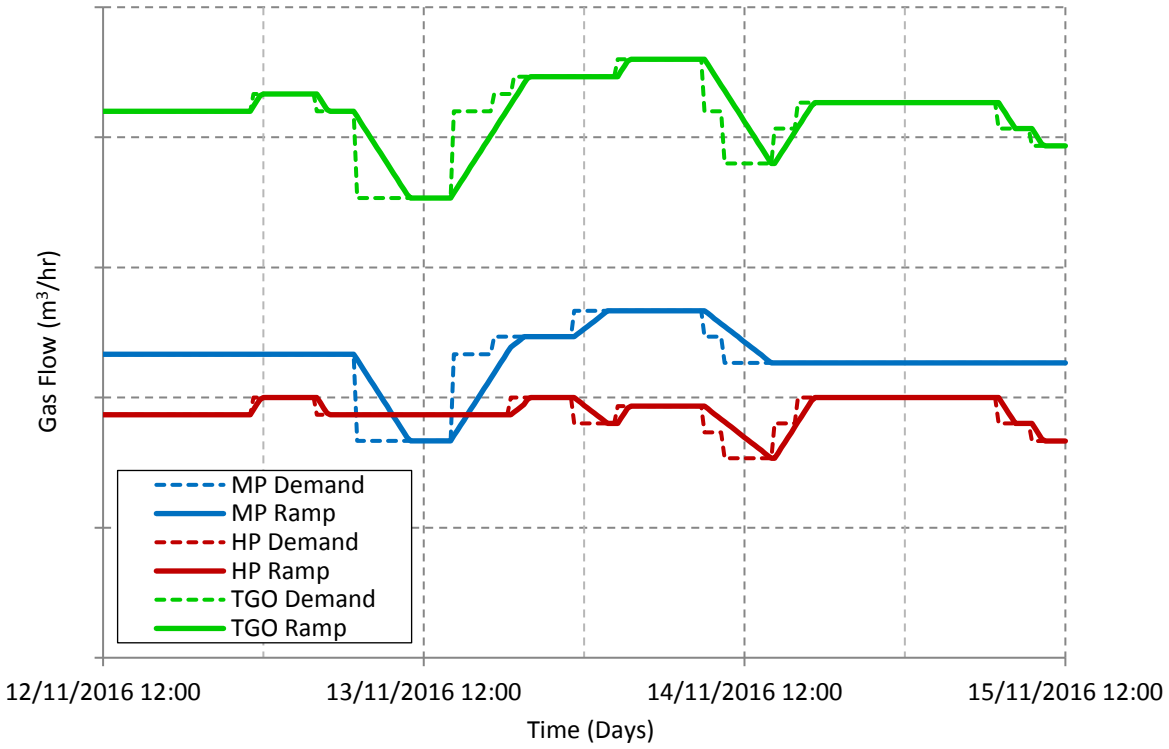

Figure 3: Plot of customer MP and HP GO and the sum TGO demand requests ($F_{GO,MP\ REQ}$, $F_{GO,HP\ REQ}$) and the corresponding calculated contractual ramping customer demands ($F_{GO,MP\ RAMP,t}$, $F_{GO,HP\ RAMP,t}$) over three days.

Figure 3 demonstrates how the TGO ramping demand (the sum of MP and HP demands) has the same gradient at all times but where there are order changes of both MP and HP, the individual ramping demands are halved. Large ramps can take place over several hours with operators required to alter production set point targets arbitrarily to meet customer demands

at all times. No orders are communicated in advance due to frequent unpredictable customer site breakdowns, which makes scheduling difficult and often results in new demands being requested before the ramping demands reaches the previous requested order, causing a reverse of the network reconfiguration from that point.

Figure 4 shows the actual metered supply of MP and HP GO over the typical three days of ramping demand in Figure 3 while Figure 5 shows the actual compression network configuration selected by the process operator. Liquid oxygen consumption, as shown by large spikes in metered HP flow, occurs when pipeline pressure reduces to an unsustainable point during undersupply caused by not meeting the required demand specifications or over consumption by the customer compared to their order request. LP spill is caused by over-production and non-optimal compression reconfiguration timing, e.g. on day three when compressor c1 is turned off. Temporary gas oversupply caused by liquid vaporisation is excluded from customer bills but the liquid volume is charged if the network is deemed to be meeting the ramping demand order. Optimisation of the ASU and compression network configuration aims to reduce the overall power consumption (including periods of over-supply) and minimise losses by ensuring the ramping demand is met at all times.

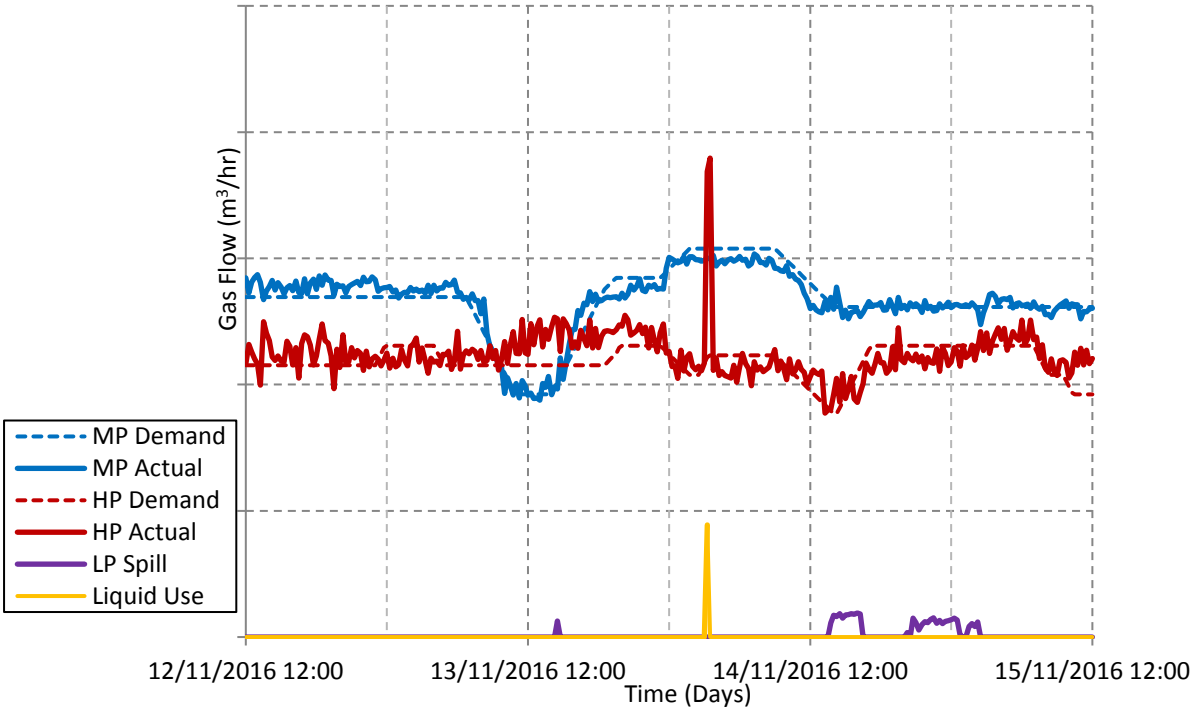

Figure 4: MP and HP GO ramping demands (over a three day period) and the actual metered supplied flows. LP GO spill from valve v1 and liquid oxygen vaporisation F_s are shown.

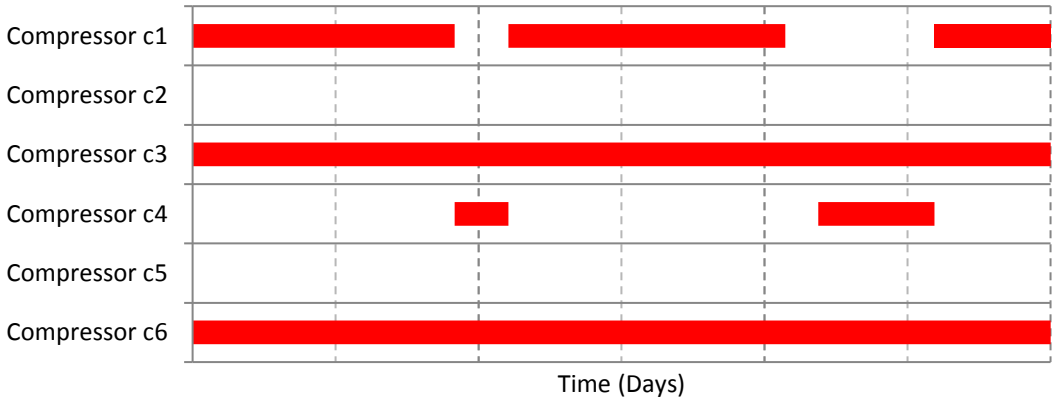

Figure 5: Gantt chart of actual process operator compression network management over the three day trial.

2.0 Site-wide optimisation

The aim of the site-wide optimisation (SWO) scheme is to determine the optimal flows of oxygen gas throughout the network in order to minimise total operating costs for a given customer demand combination under the operating conditions at steady-state (the end of any required ramp). The outputs of the optimiser are the optimal ASU production rate set points and the running requirement of each compressor within the network. To implement the optimisation strategy a mathematical representation of the oxygen gas network may be constructed which consists of three components **(a)** steady-state material balance relationships which are used to ensure an optimal configuration meets customer demand, **(b)** a description of the total operating cost of the gas supply network and **(c)** models of the power consumption of each of the ASUs and compressors within the network subject to optimised throughput and current process operational data. While previous work has developed nonlinear mixed integer dynamic optimisation strategies for SWO, these are difficult to solve in a reasonable time frame, as described in Pattison et al. (2016). Here we deploy linear mass balance relationships and piecewise linear empirical power consumption models to develop a MILP optimisation framework to achieve the economic efficiency goals.

2.1 Steady-state material balances

Material balances are used as production constraints within the optimisers to ensure mass balances equalise, gas demands are met by the compression network and liquid oxygen make meets the operational requirements. In order to define the material balance relationships it is assumed that there are no dynamic gas losses due to spill from machines or fouling. Furthermore, as the network is relatively local and pipelines between machines short, pipeline friction losses are not modelled. At any given discrete time point, the material balance relationships can therefore be defined based upon the steady-state temperature and pressure standardised flowrates through the various components of the network (for points highlighted in Figure 1),

$$F_{GO,u1} + F_{GO,u2} = F_{GO,c1} + F_{GO,c2} + F_{GO,c3} + F_{GO,c4} + F_{GO,v1} \quad (2)$$

$$F_{GO,MP} = F_{GO,u3i} + F_{GO,c1} + F_{GO,c2} + F_{GO,c3} - F_{GO,c5} - F_{GO,c6} + F_{GO,v2} \quad (3)$$

$$F_{GO,HP} = F_{GO,u3ii} + F_{GO,s} + F_{GO,c4} + F_{GO,c5} + F_{GO,c6} - F_{GO,v2} \quad (4)$$

$$F_{TLO} = F_{LO,u1} + F_{LO,u2} + F_{LO,u3} \quad (5)$$

Each mass balance component has an operating range determining the minimum and maximum flow production or processing ability of the ASUs and compressors which can be discovered by analysis of empirical data. Process operation limits are known to be a function of compressor size, discharge pressure and ambient conditions, Kurz et al. (2010). Capacity limits are used within the optimisers as operational constraints to ensure outputs are feasible. For air separation units, the production capacity range is between the lowest and highest sustainable production flows of liquid and gaseous oxygen, determined by the column and air compressor size at steady-state. For the compressors, minimum throughputs are determined by the anti-surge control schemes and maximum throughputs relate to compressor design, with operational data showing the limits of flow change with the discharge pressure of the machine. In order to model the variation, polynomial regression fits using data on the edge of the operating regions may be used to capture the relationships between flow and discharge pressure i.e.,

$$F_{GO,cj}^{min}(P_{Dj}) \leq F_{GO,cj} \leq F_{GO,cj}^{max}(P_{Dj}) \quad (6)$$

2.2 Network operating cost model

The total network operating cost, J_{SW} (£/hr), is a function of the sum of compressor and air separation unit power multiplied by the cost of power, C_{kw} (£/MWh) plus the cost of back-up supply, C_s (£/m^3), when a backup flow, F_S, is required plus the cost of producing LO, C_{LO} (£/m^3),

$$J_{SW} = C_{kw} \cdot \left(\sum_{j=1}^{6} W_{cj} \cdot \delta_{cj} + \sum_{j=1}^{3} W_{uj} \cdot \delta_{uj} \right) + C_s \cdot F_s + C_{LO} \cdot F_{TLO} \quad (7)$$

The binary variables, $\delta_{cj} \in \{0,1\}$ and $\delta_{uj} \in \{0,1\}$ are introduced into the cost function in order to remove machines from the network when not required. A zero indicates the machine is off (therefore removing the respective power term from the operating cost) and one multiplied by the power indicates it is on. For SWO, the cost of power is taken to be the average spot market price plus non-commodity costs such as charges and taxes, μC_{kw}, the price of liquid back up consumption is taken to be the average cost of its generation, μC_s, and the cost of making LO is the average cost of production, μC_{LO} , which involves consuming liquid nitrogen.

2.3 Empirical models of power consumption

The power consumption of the product and ASU air compressors may be estimated through the development of multivariate empirical (data-based) models using large pre-screened data sets covering the full range of network component operation. The general structure of the models is shown in Adamson et al. (2017),

$$\widehat{W}_{cj} = f(F_{GO,cj}, P_{Dj}),\ \widehat{W}_{uj} = f(F_{GO,uj}, F_{LO,uj}) \quad (8)$$

where the power consumption of compressors and ASUs is known to be a nonlinear function of gas throughput or production rate and discharge or column pressure and is modelled as such. Ideally, the model structure of an ASU would be identical to that of the compressors; however, as column pressure is directly related to the total oxygen production rate, unlike the pipeline discharge pressure of compressors, the current column pressure cannot be used to estimate the ASU air compressor power consumption at the optimised flow. Therefore, ASU air compressor power estimation models are univariate, only considering combined production flow of GO and LO from the ASU.

2.4 Site-wide optimisation to meet demand specifications

For a particular demand ($F_{GO,MP\ REQ}$, $F_{GO,HP\ REQ}$), equation 7 may be minimised by manipulating the binary variables $\delta_{cj} \in \{0,1\}$, $\delta_{uj} \in \{0,1\}$, the flows of gaseous oxygen through the compressors, $F_{GO,cj}$, the product flows of gaseous and liquid oxygen from the ASUs, $F_{GO,uj}, F_{LO,uj}$ and the flows F_s and F_{TLO}. This minimisation is performed with respect to the material balance constraints, equations 2-5, the additional flow range limits (which are multiplied by the corresponding binary variable to deactivate the constraint when the network component is not required), equation 6, and uses the regression models defining the power consumption relationship, equation 8. Using nonlinear regression models defines a MINLP, e.g. see Adamson et al. (2015), Xenos et al. (2015) and Puranik et al. (2016), however, it was shown in Adamson et al. (2017) that, through the use of piece-wise linear models to accurately estimate machine power consumption, the problem can be re-cast as a computationally efficient MILP (see section 4.0).

To demonstrate the benefits of SWO, referring to the operational period displayed in Figure 4, SWO was used to determine the optimal ASU production rate targets for each requested demand. The demands were within the production range of two ASUs throughout the three day period therefore only ASUs u2 and u3 were running. Figure 6 shows the optimiser output providing optimal ASU production flow rates and the optimal total predicted power consumption of ASUs and compressors (dotted lines). This is compared to the actual production flow rates from the two ASUs and the actual metered power of the overall ASU and compressor network.

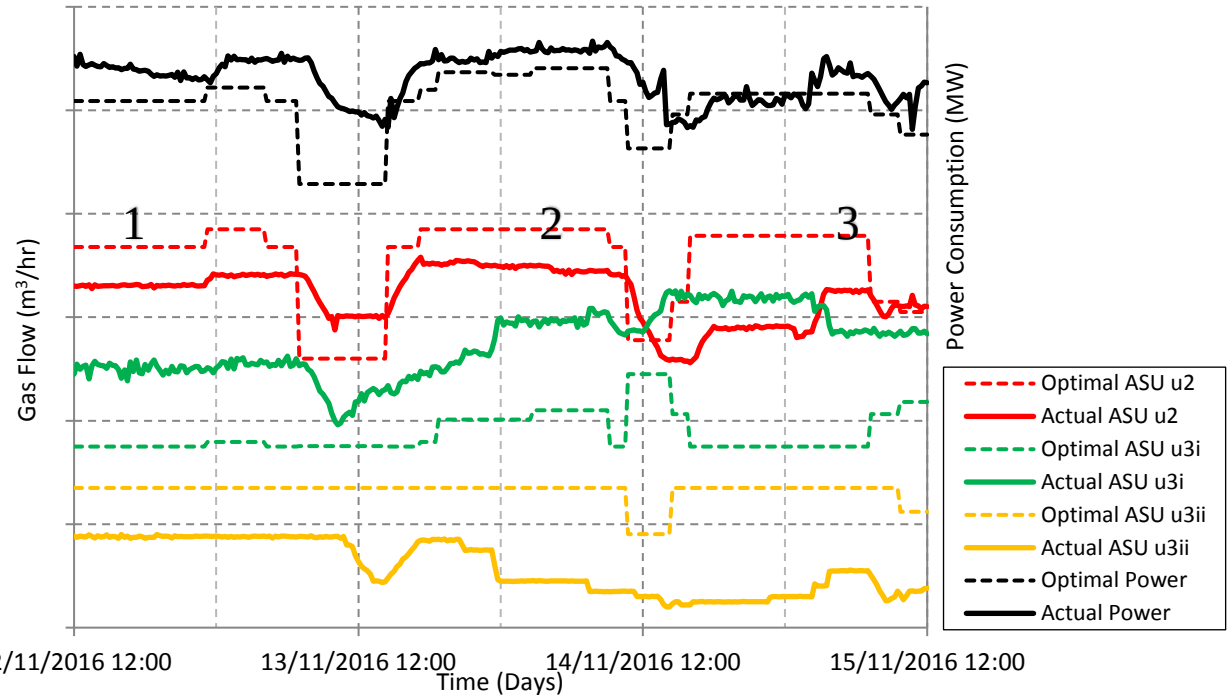

Figure 6: Site-wide optimiser output of ASU production flow rates and estimated optimal power consumption for the customer demand requests over the three day period shown in Figure 4 (dotted lines) trended in conjunction with the actual metered production flows and network power consumption.

For steady-state points 1-3 in Figure 6, it may be observed that the actual ASU flows do not correspond to the optimal production distribution for the vast majority of the time, and as the typical majority (80-90%) of total network power is consumed by air compressors feeding the ASUs, the optimal production distribution of ASUs is the key factor in network optimisation. Further, where power consumption is below the predicted optimal, undersupply is occurring risking liquid back up requirement. It may also be observed in Figure 6 that ASU u3 is constantly producing MP preferentially to HP gaseous oxygen. This is because of the current operating logic incorrectly assumes HP production is much less efficient. In addition, it is observed in Figure 6 that actual changes in ASU production flow rate were often faster than the recommended safe limits, potentially risking unsafe periods of ASU operation.

By comparing the actual metered network power consumption with that of the optimiser output at each point, SWO suggests that an average power cost saving of around 5% can be achieved at each steady-state point. However, to achieve this benefit, the operator is still required to manipulate the network to the suggested optimum configuration. This may lead to inefficient network manipulation consuming additional power than required or incurring losses. In addition, Figure 4 shows that steady-state conditions, i.e. where the ASU production rates are not changing, only occur up to around 45% of the time. Enhanced operational benefits would therefore be obtained if the transitional periods which arise because of the overall network and ASU safe ramping policy were accounted for, allowing

optimal reconfiguration of the network. Therefore, as opposed to SWO when a demand change occurred, it was configured to optimise plant operation every 15 minutes using the ramping demands calculated for each time period. However, SWO often suggested large changes in ASU production rates and compression changes which are not realistic within a 15 minute period due to safe ASU ramping limits and compressor change requirements. This is because the ASU production distribution and compressor configuration can be fixed for a wide range of operation but when demands move outside of operating range, a large reconfiguration may be required. In other words, SWO is highly susceptible to small changes in customer demand, power pricing and compressor discharge pressure requiring further development and additional optimisation layers for a real-time application. Without an optimal end point target schedule for production loading and compression configuration, the optimiser would focus on meeting the changing ramping demands without considering the wider implications of the change on future network configuration or incurred losses.

3.0 Real-time optimisation

Generally, in process control and automation applications, a multilayer (hierarchical) control system structure is used, Tatjewski (2010). Normally this process control hierarchy is comprised of three layers; **(a)** the basic control layer – generally comprising conventional proportional-integral derivative (PID) control laws which are installed to ensure safe and reliable operation of the process, **(b)** the supervisory or advanced process control layer - MPC laws which are used to optimise the future control policy and **(c)** a steady-state optimisation layer. The purpose of RTO is to maximise profits of a dynamically changing system by manipulating current variables to maintain the optimum set of conditions, Love (2007), and bridge the calculation frequency gap between the high-level scheduling optimisation schemes and the control layers. Where control aims to reduce process upset and the effect of disturbances by manipulating process variables to maintain the process at the set points, optimisation aims to keep the process at optimum and make changes when constraints are violated or the process moves from optimum.

In this work, we use a multi-layer optimisation and control hierarchy shown in Figure 7. As with the majority of multi-layer control system structures discussed in the literature, each layer is clearly distinct in that they work at different sampling frequencies (the top layer operating with a large sampling frequency and the sampling frequency of subsequent layers getting progressively faster). Given changes in required demand, a SWO cost function is solved in order to obtain the most economically efficient ASU operation as well as the configuration of the network of compressors – see earlier results – however, it merely provides the plan (or blueprint) for the required operation. The second layer, which is the RTO layer, combines conventional economic optimisation with the requirement that the site-wide targets should be achieved (where possible) over a period of operation as dictated by the ramping rate policy of the ASUs. This combines the economic cost function with additional terms that ensure target compliance and penalise excessive moves in configuration (akin to MPC algorithms but operating at a much lower frequency). In essence, RTO provides an additional set point optimiser for the ASUs and a compressor configuration manager ensuring contractual ramping customer demands are met at all times. This provides the interface to the levels of the control hierarchy which constitute the advanced and local control schemes which continue to handle the underlying high frequency process disturbances. Where optimisation strategies cannot be combined with existing control strategies due to the well-established proprietary status (unlike Pattison et al. (2016)) and if it can be assumed that the demand change and power price disturbances are slow-varying, then the optimisation problem may be solved at a much slower rate than that of the lower level control system.

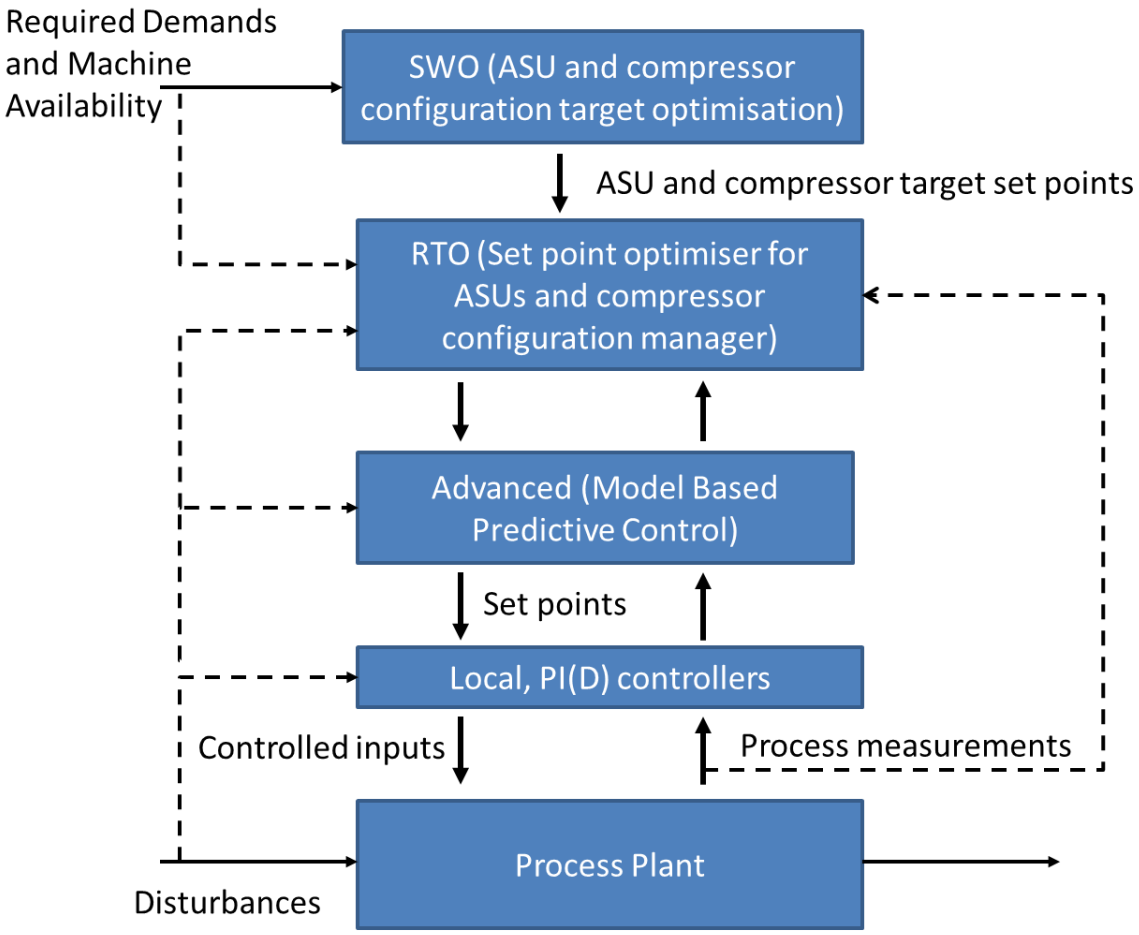

Figure 7: Proposed network operation strategy demonstrating the integration of the SWO and RTO tools with the existing control hierarchy. SWO is event-driven when the solver detects a change in customer demands or machine availability. The end point targets are exported to a periodically running RTO which exports the optimum real-time network configuration subject to the current ramping demand and power price, subject to the current network configuration. The MPC layer imports the set point targets and controls the underlying process managing the effects of process disturbances.

This work, as apposed others in the field, fully implements the SWO and RTO strategies using Microsoft Excel's Solver add-in program with visual basic coding to automatically import required data values, solve the optimisation problem using the simplex linear algorithm and export the data values back to a data historian for monitoring and control purposes. The development within an accessible and additional license-free optimisation software package allows for greater compatibility and understanding by plant management, permitting intuitive use by process operators and for models to be easily updateable in the future. This allows the RTO outputs to be evaluated in an isolated environment where;

a) Customer demands, machine availability, liquid make costs and power pricing are input to the data historian manually or by automated import tools.
b) Current process plant conditions are fed to the data historian automatically.
c) The site-wide optimiser imports all required information and solves for the optimal end point for the current customer demand combination and exports the site-wide optimal ASU production rates and compression configuration to the data historian.
d) The real-time optimiser imports all target set points, plant information and the previous optimiser result and solves for the optimal next step after calculating the required ramp demand.

e) Set point targets for ASU production rates and the compression configuration are exported to the data historian along with forecast power consumption for trend analysis between the optimiser outputs and the actual network configuration and power.

f) When integrated with the existing control layers, MPC will import the set point targets from the data historian, error check and write to the local controllers.

The interface is managed by a data historian scheduling tool which runs to calculate the ramping demands and open the RTO tool every 15 minutes, 24 hours a day. SWO is carried out automatically when a gaseous or liquid demand request or machine availability change is detected by the scheduler, an event-driven rescheduling strategy, to determine new set point targets for the lower RTO layer. RTO is carried out periodically for every time step on a rolling horizon basis with the production distribution and compressor configuration used to inform operators to move the current network set points. After testing, the 15-minute time step was deemed sufficient for the underlying MPC scheme to control process dynamics and achieve the ASU production set point targets before the next step is calculated.

3.1 RTO cost function

The information flow between the two optimisers is shown in Figure 8. This shows the demands sent to the SWO layer and RTO layer are different during a ramp as SWO only considers the end point actual demands ($F_{GO,MP\ REQ}, F_{GO,HP\ REQ}$) and does not need to run unless a demand change or machine availability change occurs. The RTO layer considers inputs detailing the point in the ramp ($F_{GO,MP\ RAMP,t}, F_{GO,HP\ RAMP,t}$), target set points from SWO ($\delta_{cj}^{sw}, \delta_{uj}^{sw}$, $F_{GO,cj}^{sw}, F_{GO,uj}^{sw}$, $F_{LO,uj}^{sw}, F_{s}^{sw}$, F_{TLO}^{sw}), current plant data, such as compressor discharge pressure (P_{Dj}^{RT}) for machine power consumption estimation, and spot market power price ($C_{kW,t}$). Where the external spot power price market conditions change, a trade-off must be made between power and liquid consumption to ensure the network is meeting the customer demand at all times during peak pricing and opportunities for cheaper LO production during off-peak periods. As the liquid make prices change, these costs can also be fed into the RTO to model the changing prices of liquid consumption ($C_{s,t}$, $C_{LO,t}$). The outputs of the real-time optimiser, i.e. the network component requirements – as indicated by the values of the binary co-efficients (δ_{cj}^{RT}, δ_{uj}^{RT}) and production or throughput flows ($F_{GO,cj}^{RT}$, $F_{GO,uj}^{RT}$, $F_{LO,uj}^{RT}$, F_{s}^{RT}) are the set points that are either directly sent to the MPCs or used to inform operators that a compression selection change is required.

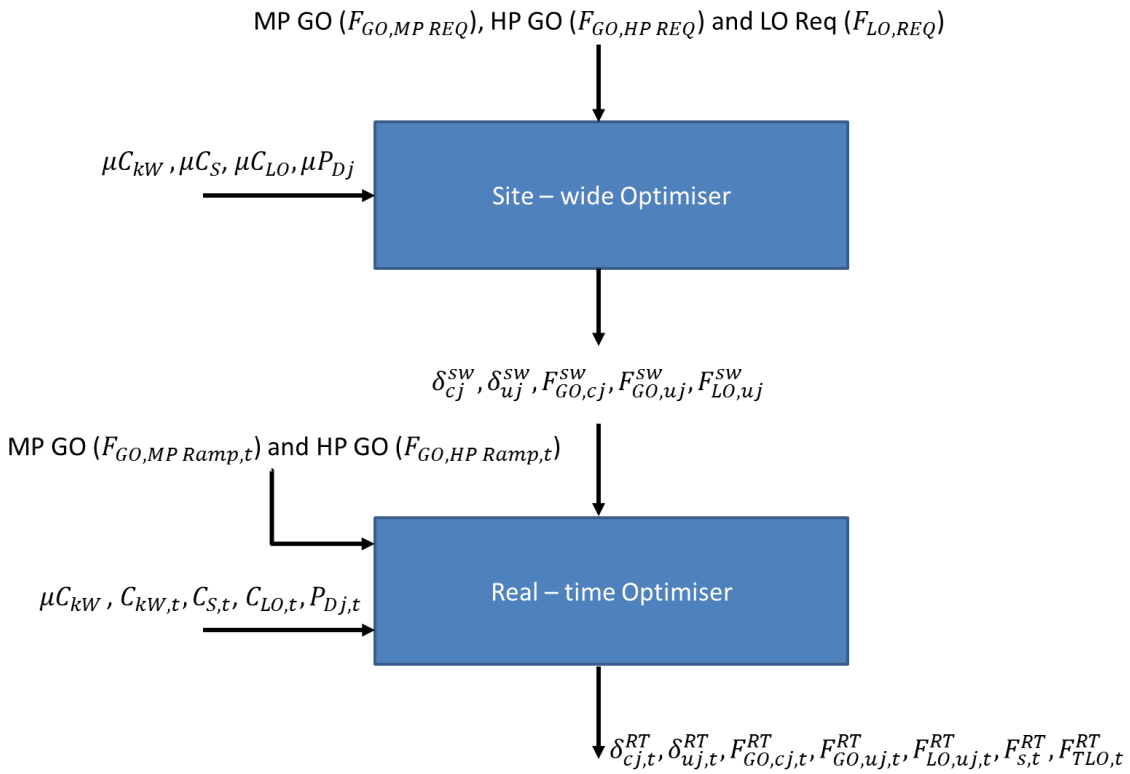

Figure 8: Optimisation data feed map showing the cost function inputs and exports from each of the automated optimisation tools. The site-wide optimiser imports current demands and exports the targets to the real-time optimiser. The real-time optimiser solves using current ramping demand, power price, pressure and end point targets to provide the real-time optimal ASU production load distribution and compression configuration.

The objective of the RTO layer is to minimise the error between the four end point optimal ASU production flows and the compression configuration arrangement (as optimally determined by SWO given a change in demand) while simultaneously penalising compressor and ASU configuration changes during the transition of the network configuration as a consequence of the contractual ramping constraints by minimising the cost function,

$$J_t = C_{kW,t} \cdot \left(\sum_{j=1}^{6} W_{cj} \cdot \delta_{cj,t}^{RT} \right) + \mu C_{kW} \cdot \left(\sum_{j=1}^{3} W_{uj} \cdot \delta_{uj,t}^{RT} \right) + C_{s,t} \cdot F_{s,t}^{RT} + C_{LO,t} \cdot F_{TLO,t}^{RT} + J_{T,t} + J_{S,t} + \varphi \cdot F_{GO,v1,t} \tag{9}$$

It is noted that the RTO cost function is simply an extension of the SWO strategy. As the site-wide optimiser is formulated as a computationally efficient MILP, there are significant benefits as the underlying models are identical, eliminating the model mismatch often observed between the scheduling and optimisation layers, Pattison et al. (2016). The first two summation terms give an estimation of network power consumption and, in addition to the price of power, LO consumption and LO make, forms the economic objective for minimisation. Values of μC_{kW}, $C_{kW,t}$, $C_{s,t}$ and $C_{LO,t}$ are fed into the optimiser in real-time at time 't' and all steady-state mass balances and customer ramping demands are met at all times by manipulating the ASU production rates and compression configuration. Only compressor power is multiplied by live spot market power as these machines are the only flexible loads exposed to changes in power price. In our work, ASUs are not considered flexible as their power is hedged on a different market which can be assumed to be the average spot market cost plus taxes and levies, i.e. using the same average power price value as with SWO, and are primarily flexed to meet changing gas demands.

In comparison to equation 7, there are three additional terms in the cost function. The first is given by,

$$J_{T,t} = \rho_1 \cdot \left(\sum_{j=1}^{4} \left| F_{GO,uj}^{SW} - F_{GO,uj,t}^{RT} \right| \right) + \rho_2 \cdot \left(\sum_{j=1}^{6} \left| \delta_{cj}^{SW} - \delta_{cj,t}^{RT} \right| \right) \quad (10)$$

As only ASUs production rates can be input at set points to the lower level MPC scheme and compressors will load up automatically with increasing suction pressure unless capacity limits are reached, then a compression change is required as suggested by the optimiser. SWO is used to produce optimal end point ASU production rates for each GO flow ($F_{GO,uj}^{SW}$) and whether each compressor is required ($\delta_{cj}^{SW} = 1 \; or \; 0$) based on predicted flows optimal flows from the site-wide optimiser. The objective is then, to minimise the discrepancy between the optimal site-wide values and those obtained by RTO. Minimisation of the absolute difference (rather than the more traditional error squared criteria used in the development of MPCs) allows linearisation of the cost function and subsequent implementation via MILP (discussed in section 4.3). The weightings are used to influence the relative importance of the terms in the cost function, i.e., the value of ρ_1 may be specified as being relatively large (when compared to ρ_2) to ensure the network reaches the target production rates of the ASUs quickly. Therefore ρ_1 will encourage the value of $(F_{GO,uj}^{SW} - F_{GO,uj}^{RT})$ to be on the ASU ramp constraint boundary (at each iteration of the real-time optimiser) unless this is not required to meet the demand order due to load sharing with other ASUs or network change is required, penalised in the second additional term. Where demands are not met by ASU production decreases or increases alone, liquid back up supply or spill is required to meet the shortfall in the customer demand combination or ensure mass balances equalise, but this is penalised by additional terms in the cost function.

The second additional term included in the RTO cost function penalises the switching on or off of the compressors and ASUs until a certain energy cost threshold is exceeded. This is achieved by referencing the previous optimisation step results and penalising change. The switching costs are added to the cost function as (where $\delta_{uj,t}^{RT}$ and $\delta_{cj,t}^{RT}$ is a binary variable that indicates whether ASU *uj* or compressor *cj* should be on or off at time '*t*' and $\delta_{uj,t-1}^{RT}$ and $\delta_{cj,t-1}^{RT}$ is the previous on/off decision for the same ASU and compressor),

$$J_{S,t} = \sum_{j=1}^{3} \left| \delta_{uj,t}^{RT} - \delta_{uj,t-1}^{RT} \right| \cdot \sigma_{uj} + \sum_{j=1}^{6} \left| \delta_{cj,t}^{RT} - \delta_{cj,t-1}^{RT} \right| \cdot \tau_{cj}(\mathrm{P_{Dj}}) \quad (11)$$

The weighting terms σ_{uj} and $\tau_{cj}(\mathrm{P_{Dj}})$ represent the start-up and shut down costs allowing RTO to ensure any required network transitions occur at the minimum overall cost but also ensuring a reduced frequency of alterations in ASU plant and compressor configurations, so to reduce operator workload and incurred maintenance requirements. For the ASUs and compressors, the cost of starting or stopping is the power wasted before gaseous oxygen production or flow throughput rate is stable. The penalty function can be weighted differently subject to the ASU size or compressor type, i.e. centrifugal or reciprocating[2], and whether the network component is being turned on or off. Reconfiguration of compression arrangement by switching them on or off can take place in the time between optimisation steps.

[2] Reciprocating compressors load up much more efficiently than centrifugal compressors and are therefore penalised less.

A change in ASU configuration is discouraged using a large weighting (σ_{uj}) as alterations in ASU configuration should be avoided until the production rate range requires a change. Starting an ASU requires significant input from operators and a period of several hours of abortive power. Stopping an ASU is relatively quick, but the costs incurred in restarting are significant. In comparison, the general form of the weighting functions used in this work for the compressors (τ_{cj}) are given by,

$$\delta_{cj,t}^{RT} - \delta_{cj,t-1}^{RT} = 1, \tau_{cj} = h(\mathrm{P_{Dj}}),$$

$$\delta_{cj,t}^{RT} - \delta_{cj,t-1}^{RT} = -1, \tau_{cj} = g(\mathrm{P_{Dj}})$$

The first term (h) describes the cost of a compressor being turned on, while the second (g) a compressor being turned off. The weightings are described as a function of current machine discharge pressure, $h(\mathrm{P_{Dj}})$ or $g(\mathrm{P_{Dj}})$, to avoid risk of liquid consumption, and/or product spill. Turning a machine off should be weighted heavily if it is likely to cause liquid use (by lowering customer pipeline pressure) or LP spill (if excess gas cannot be processed by the network and is therefore vented to atmosphere). Values are removed from this work due to proprietary information detailing the costs of compressor change overs, however, Figure 9 shows how the weighting can dynamically change based on the real-time discharge pressure.

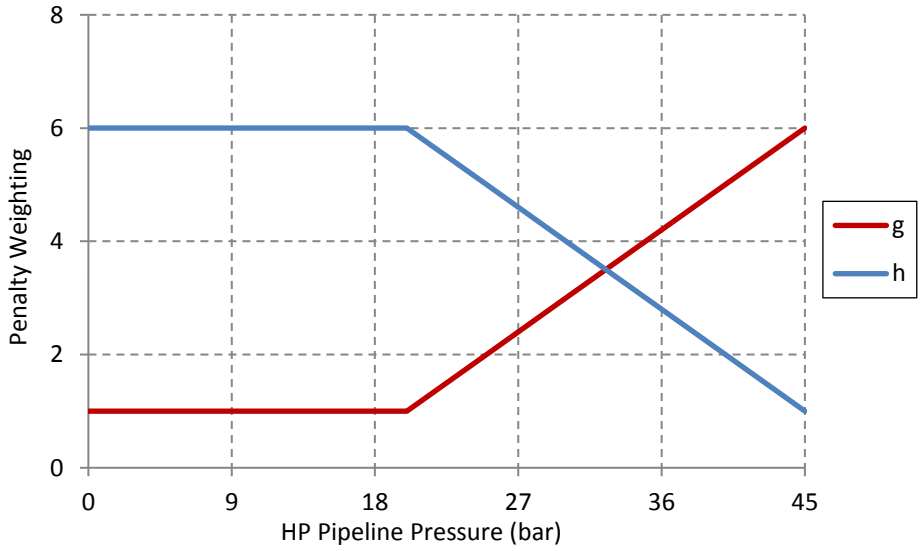

Figure 9: Penalty weighting of compressor start and stop of compressors c1, c5 and c6 as a function of HP pipeline pressure showing how weightings change with discharge pressure.

The final additional term in equation 9 is used to penalise against LP GO spill. SWO does not penalise the use of product spill, as spilling product may be cheaper than making LO or a different compression configuration and the cost is included in the ASU power costs. However, during RTO, spill during transitions in demand suggests that compressors may have been turned off early in order to deliver a power cost saving or that oversupply has occurred rather than ramping down all ASUs to meet the ramping demand. It is preferential to penalise product spill to ensure either ASUs are ramped down to meet the customer order or LO make is increased. Therefore, an additional cost function component ($\varphi \cdot F_{GO,v1,t}$) is added to mitigate against release of product.

3.1.2 Ramping limits

To ensure ASUs are always ramped safely, an additional tighter band of ASU flow constraints, shown in equation 12, are added. Each ASU production flow $F_{uj,t}^{RT}$ now must be within the safe ramping limits as defined by plant managers (discussed in section 1.3), $\left(\frac{dF_{GO,uj}}{dt}\right)_{max}$, of the previous optimiser output or current network positon, $F_{GO,uj,t-1}^{RT}$. The constraints ensure all ASUs safely adhere to ramping limits between optimisation steps whilst the overall network mass balance constraints ensure the ramping customer demand is met by all ASUs, even if it requires the ramping of an ASU away from its steady-state optimal to avoid losses.

$$F_{GO,uj,t-1}^{RT} - \left(\frac{dF_{GO,uj}}{dt}\right)_{max} \leq F_{GO,uj,t}^{RT} \leq F_{GO,uj,t-1}^{RT} + \left(\frac{dF_{GO,uj}}{dt}\right)_{max} \quad (12)$$

4.0 Linearisation of the cost functions to define an MILP

To define a MILP it is necessary to **(a)** develop piecewise linear models that provide an estimate of power consumption of each component in the network and **(b)** linearise all the nonlinear terms within the site-wide and real-time optimiser cost function. In Adamson et al. (2017), the development of a piece-wise linear modelling strategy to estimate machine power consumption was discussed. In summary, a nonlinear optimiser is used to iteratively minimise regression error and determine the optimal linear model co-efficients, model break-point positions and number of pseudo-machine models. The resulting models are validated on a second data-set and the piecewise linear model that minimises the validation error chosen as the optimal model. Briefly, the power consumption of each of the network components may be developed as follows, with further models described in our previous paper.

4.1 Multivariate piece-wise linear modelling of the compressors

Each piece-wise segment of the compressor data are regressed to the following model (where 'k' is the kth piecewise linear model and $\hat{b}$ constants are regression parameters),

$$\widehat{W}_{cj,k} = \hat{b}_{0,k} + \hat{b}_{1,k}F_{GO,cj} + \hat{b}_{2,k}P_{Dj} \quad (13)$$

For the compressors, the discharge pressure is used to define the model breakpoints, i.e. denote the points at which one model begins at and the previous one ends. To develop the models, plant data was pre-screened and erroneous data points indicating non-running, non-steady-state or operation outside normal operating range were eliminated. The empirical model defines 'pseudo-machine' models, each with a lower and upper pressure bound, i.e. for the purpose of building the SWO and RTO cost functions the model of compressor c1 may be considered as two separate (linear) machines with the appropriate pseudo-machine being determined by the current discharge pressure. An example of such is the multivariate piecewise linear model for compressor c1, shown in Figure 10, where two multivariate linear pseudo machine models with pressure limits are used to estimate machine power consumption, given by,

$$\widehat{W}_{c1} = \begin{cases} -333.646 + 41.99P_{Dc1} + 11.35F_{GO,c1} & 14.5 \leq P_{Dc1} < 15.6 \\ -1002.95 + 83.04P_{Dc1} + 11.06F_{GO,c1} & 15.6 \leq P_{Dc1} < 16.5 \end{cases} \quad (14)$$

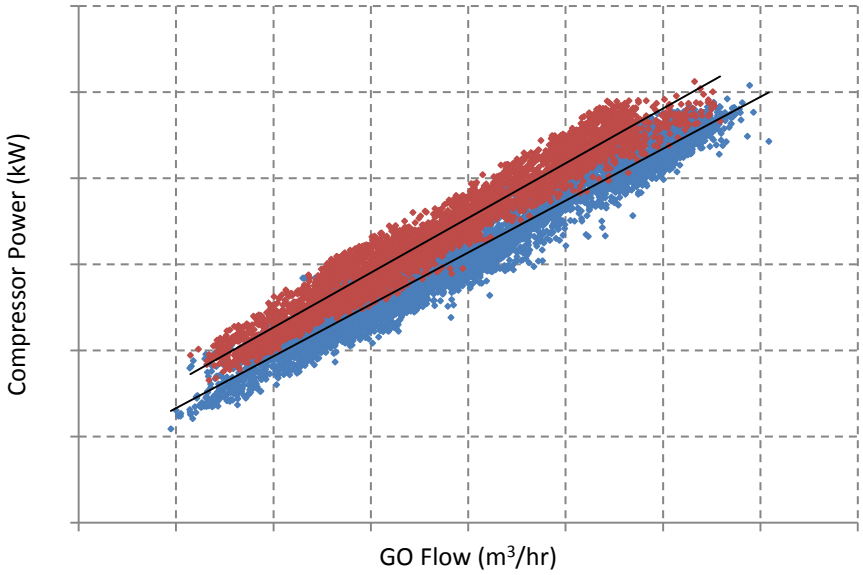

Figure 10: Model of compressor c1 showing two piece-wise linear models with a discharge pressure break point.

4.2 Univariate piece-wise linear modelling of the ASUs

Ideally, a piece-wise linear model of an ASU would use identical methodology to compressors. However, as column pressure is directly related to the total oxygen production rate, unlike the pipeline discharge pressure of compressors, the air compressor discharge pressure cannot be fed into the model to estimate the ASU power consumption at the optimised flow. Therefore, ASU piece-wise linear power models must be univariate, only considering production flow from the ASU, with flow breakpoints and are given by,

$$\widehat{W}_{uj,k} = \hat{b}_{0,k,uj} + \hat{b}_{1,k,uj}\left(F_{GO,uj} + F_{LO,uj}\right) \quad (15)$$

An example of such is shown in Figure 11 a model of ASU u3 with two pseudo machine univariate piecewise linear model with flow breakpoints.

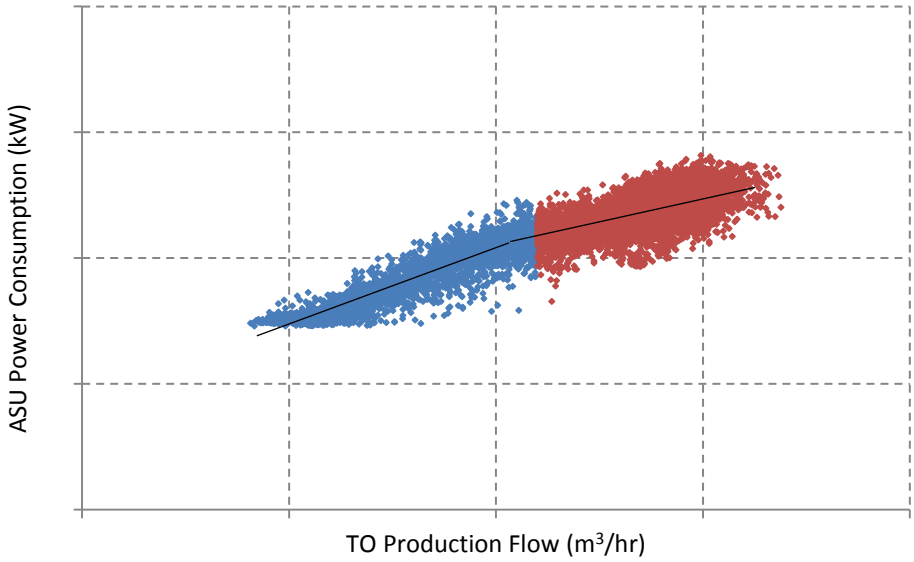

Figure 11: ASU u3 model showing two univariate piece-wise linear power models as a function of TO production rate with an ASU production flow rate break point.

The piece-wise linear models of power were trended in parallel with actual power consumption to discover a mean error (ME) of the power estimation. The typical multivariate

piece-wise modelling ME for compressors was 2% of actual power consumption and the typical univariate piece-wise linear modelling ME for ASUs was 3%. Piece-wise linear models are shown to be comparable in accuracy to the best nonlinear alternative in Adamson et al. (2017).

4.3 Cost function component linearisation

The use of the piecewise linear models alters the cost function for the SWO and the RTO with the site-wide optimiser cost function becoming,

$$J_{SW} = \mu C_{kW} \cdot \left(\sum_{j=1}^{6} \sum_{k=1}^{mj} \widehat{W}_{cj,k} \cdot \delta_{cj,k,t}^{SW} + \sum_{j=1}^{3} \sum_{k=1}^{mj} \widehat{W}_{uj,k} \cdot \delta_{uj,k,t}^{SW} \right) + \mu C_s \cdot F_s^{SW} + \mu C_{LO} \cdot F_{TLO}^{SW} \quad (16)$$

and the real-time optimiser cost function becoming,

$$J_t = C_{kW,t} \cdot \left(\sum_{j=1}^{6} \sum_{k=1}^{mj} \widehat{W}_{cj,k} \cdot \delta_{cj,k,t}^{RT} \right) + \mu C_{kW} \cdot \left(\sum_{j=1}^{3} \sum_{k=1}^{mj} \widehat{W}_{uj,k} \cdot \delta_{uj,k,t}^{RT} \right) + C_s \cdot F_{s,t}^{RT} + C_{LO} \cdot F_{TLO,t}^{RT} + J_{T,t} + J_{S,t} + \varphi \cdot F_{GO,v1,t} \quad (17)$$

The network cost is therefore a sum of each machine power, which is a sum of all the pseudo-machine model powers ($k = 1, \dots, m$), multiplied by the cost of power. To prevent the optimiser selecting multiple pseudo-machines simultaneously, mutually exclusive constraints are then added for the sum of binary co-efficients for each machine with the sum of the co-efficients exported for the compressor requirement. For example, for the '*mj*' binary co-efficients of models for compressor '*j*', in the RTO cost function is given by,

$$\delta_{cj,t}^{RT} = \sum_{k=1}^{mj} \delta_{cj,k,t}^{RT} \leq 1 \quad (18)$$

Prior minimisation of the optimiser cost function (equation 17); the plant discharge pressures are imported. The current discharge pressure is used to 'select' the appropriate pseudo-machine model, k, and, with no further updates, the discharge pressure of each unit remains constant during optimisation therefore the only decision variables in the piece-wise models are flow and the associated binary co-efficients. As the multiplication of the binary variable and flow variables introduces combinational nonlinearity, in order to use a MILP solver they must be removed. The combination of the estimated power model and the binary variable gives,

$$\widehat{W}_{cj,k} = \left(\hat{b}_{0,k} + \hat{b}_{1,k} P_{Dcj} \right) \cdot \delta_{cj,k,t}^{RT} + \hat{b}_{2,k} F_{GO,cj,k} \cdot \delta_{cj,k,t}^{RT} \quad (19)$$

The second term in equation 19, $\hat{b}_{2,k} F_{GO,SS,cj,k} \cdot \delta_{cj,k,t}^{RT}$ causes nonlinearity therefore an auxiliary variable $y_{cj,k,t}^{RT}$ is introduced where,

$$y_{cj,k,t}^{RT} = F_{GO,cj,k} \cdot \delta_{cj,k,t}^{RT} \quad (20)$$

and $\hat{F}_{GO,cj,k}^{min} \cdot \delta_{cj,k,t}^{RT} \leq F_{GO,cj,k} \leq \hat{F}_{GO,cj,k}^{max} \cdot \delta_{cj,k,t}^{RT}$

Auxiliary variables replace all binary and flow combinational components of both the SWO and RTO cost functions for complete linearisation benefits. The auxiliary and binary co-efficient decision variables are solved by the optimisation strategies which enable the flow range constraints to be satisfied during optimisation.

The two additional terms within equation 17, ($J_{T,t}$, $J_{S,t}$) contain absolute values which may be redefined through introduction of a further set of auxiliary variables. For example, the penalty term, $J_{T,t}$ may be written,

$$J_{T,t} = \rho_1 \cdot \left(\sum_{j=1}^{3} z_{GO,uj} \right) + \rho_2 \cdot \left(\sum_{j=1}^{6} z_{GO,cj} \right) \tag{21}$$

Which, given the constraints, $z_{G0,uj} \leq F^{SW}_{GO,uj} - F^{RT}_{GO,uj,t}$, $z_{G0,uj} \geq F^{SW}_{GO,uj} - F^{RT}_{GO,uj,t}$, $z_{GO,uj} \geq 0$ and $z_{G0,cj} \leq F^{SW}_{GO,cj} - F^{RT}_{GO,cj,t}$, $z_{G0,cj} \geq F^{SW}_{GO,cj} - F^{RT}_{GO,cj,t}$, $z_{GO,cj} \geq 0$ gives an equivalent (linearised) formularisation.

In all, the programmed RTO optimisation strategy consists of 37 piece-wise models of ASU and compressor power, 65 decision variables (24 flow auxiliary, 19 binary, 12 machine change auxiliary and 10 control law auxiliary variables) and the full 100 allowable quota of constraints permitted in the freely available version of Microsoft Excel Solver (upper and lower piece-wise ASU, compressor and pipeline capacity limits, binary integer, exclusive pseudo-machine, availability, mass balance and ramp limit constraints).

5.0 Real-time optimisation results

To demonstrate the potential operational cost savings achievable when operating the proposed RTO strategy, for the three day trial period live power pricing (shown in Figure 12), actual customer demands (shown in Figure 3) and process data, was imported by the solvers, with the calculated outputs monitored and trended in parallel with actual operation and power consumption. The difficulty in determining optimisation benefits is the lack of hindsight 'this is how we would have done it' results. Instead, we have separately tested that the optimiser output is achievable at given points within ramps and extrapolated the assumption that the gap between actual and optimised operating costs is the overall benefit of optimisation. The RTO offline simulation outputs of ASU production rates and compressor configuration from the parallel optimisation framework are shown in Figure 13 and 14 respectively.

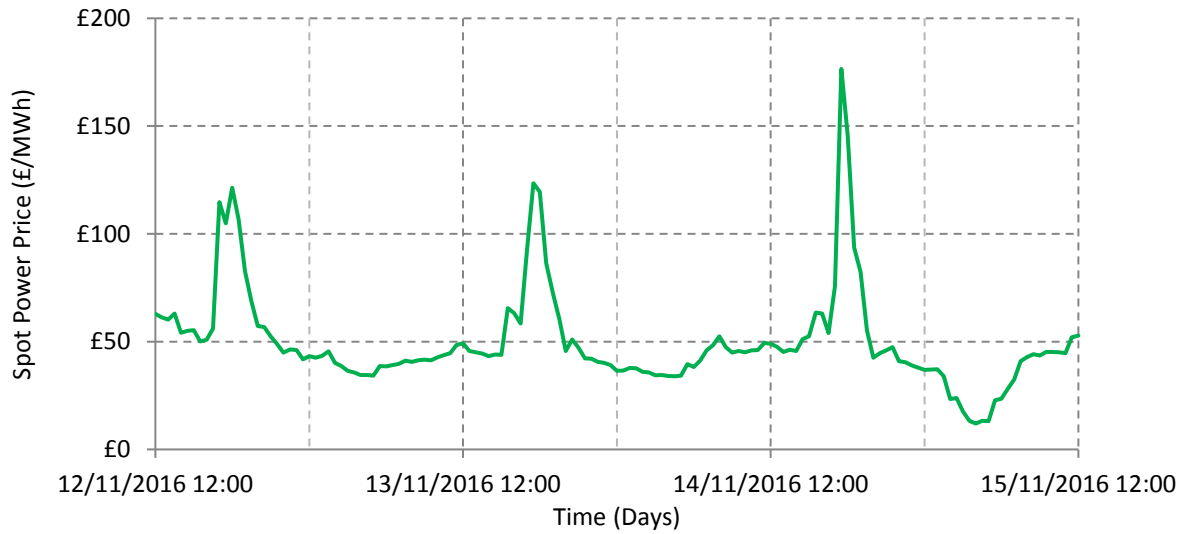

Figure 12: Spot market power pricing over the three day trial period (starting at 12:00pm on day 1).

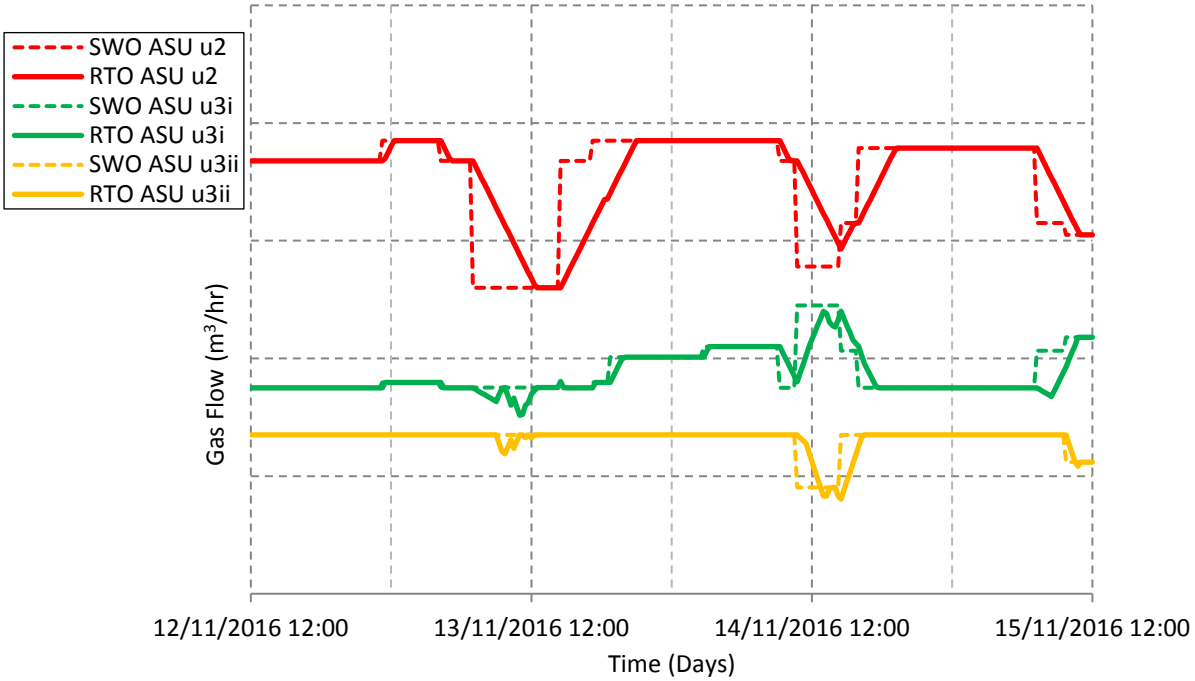

Figure 13: ASU production target outputs obtained from the RTO plotted with the SWO targets (see Figure 6) over the three day trial period.

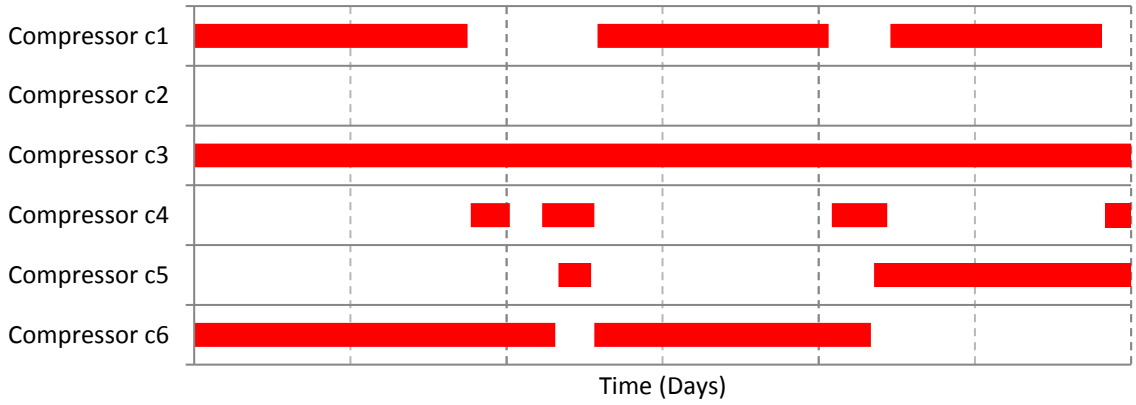

Figure 14: Gantt chart showing the real-time optimiser output indicating the running requirement of compressors over the three day trial period.

Figure 13 shows how the ASU production rates are manipulated by RTO. During ramps, ASUs can be seen aiding the ramping of another ASU to ensure LO use or spill is avoided due to the weights imposed, see ASU u3 MP/HP GO production flows changing temporarily when ASU u2 is ramping. The RTO constraints ensure all ASUs production rate changes are constrained to within their safe limits and the ramping customer demand is met at all times.

Figure 14 shows compressor c5 and c6, the MP to HP GO reciprocating compressors, are often changed with each other due to changes in pipeline discharge pressure and flow requirements. Compressors c1 and c4 are brought in and out of service as required due to the changing ramping demands. Compressor c2 is not required during the trial period. The RTO strategy achieves a reasonable number of compression changes and ensures they are changed at the optimal time avoiding spill and LO consumption.

Comparing the optimal compression configuration changes and the actual (shown in Figure 5) over the three day simulation period, the RTO output suggests compressor c4 can be turned off for a period of time early on day two to conserve power. In addition, the RTO

optimiser ensures compressor c1 is promptly swapped with c4 on day three to prevent the low pressure spill seen in Figure 4. There are more changes suggested than occurred during the real control period, especially between compressors c5 and c6, therefore the reduction in operating costs must have outweighed the penalty of changing compression which includes the increased risk-adjusted cost of maintenance and because the RTO is reacting to changes in process and power market environments.

A comparison of the actual power consumption of all ASUs and compressors without optimisation and the estimated SWO and RTO sum of ASU and compressor power (first two summations in each cost function), is shown in Figure 15. Figure 16 shows a histogram of the positive reduction in power consumption suggested by the offline optimiser when compared to the actual power used at 15 minute intervals.

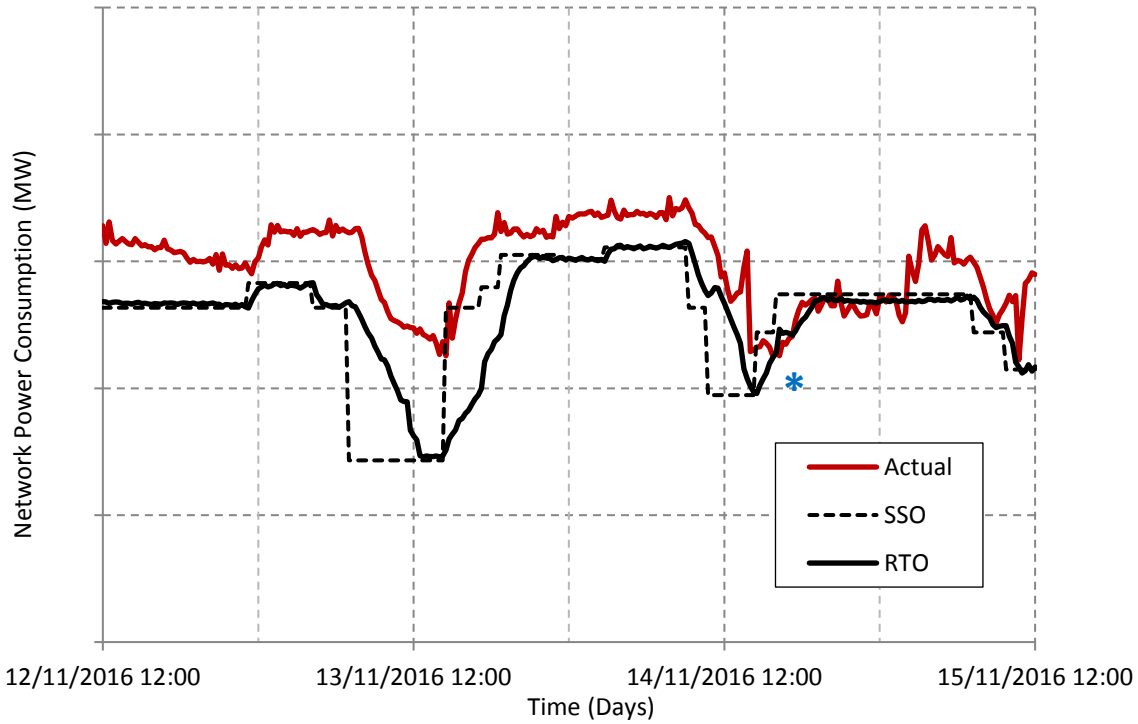

Figure 15: Estimated power consumption of SWO, RTO and actual output over the three day period.

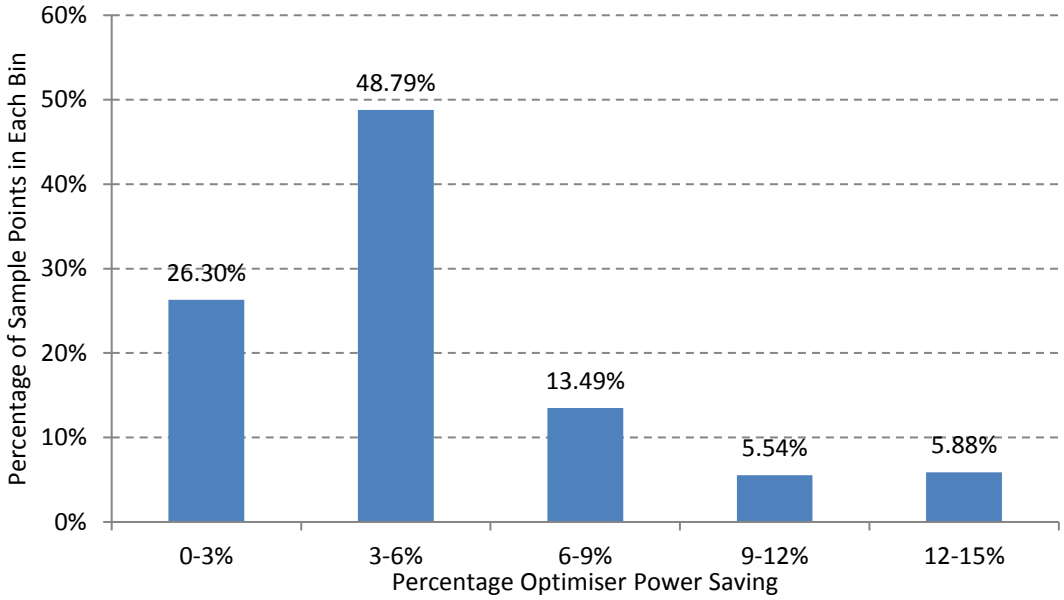

Figure 16: Probability of potential power savings suggested by the optimiser for each sample point.

Figure 15 shows a significant gap between the RTO estimated and actual power consumption of the network. For the selected three day period, the average power reduction is 4.95% of actual used with the maximum differential between actual and optimal at any discrete time point being up to 15%. Considering Figure 16, the optimiser is most frequently achieving a power saving of between 3-6% and there is a saving of over 6% around 25% of the time.

The majority of the savings can be achieved by ensuring ASU production targets meet the changing customer demand requirement. In comparison to the current manual changes of ASU production rate set points by process operators, automation (feeding set points directly to the MPC layer) would ensure required ASU ramp rates are adhered to, increasing the speed at which site-wide targets are reached. This reduces the risk of losses and over consumption of power. In some cases, the RTO estimation of power does not meet the SWO estimation; this is either due to current plant conditions affecting the calculation or a penalty function preventing a compression change.

The benefits of live feeding spot market power pricing into the RTO strategy are highlighted in Figure 15 at the point marked with a blue *. At this point, a high power pricing event is occurring, as show in Figure 12, and the overall network power consumption is briefly held constant until the price subsides. The peak price reached around £175/MWh on this particular day, with the trigger pricing for stopping compression and consuming LO on this network known to be higher, as discovered in Adamson et al. (2017).

6.0 Discussion and conclusions

In this paper a RTO strategy has been described and shown to achieve significant energy cost savings in an application to a process plant consisting of multiple cryogenic air separation units and compressors, showing that economic efficiency can be gained by an optimisation framework that is semi-empirical as opposed to using complex rigorous process models. The developed MILP optimisation scheme solves inside an automated and accessible Microsoft Excel spreadsheet environment, operating the Solver add-in simplex linear programming algorithm to return the globally optimal solution to the linear problem within seconds. In addition to providing energy savings other benefits of the RTO are that the automated system releases operator time for other tasks, such as improving overall site control and aiding network configuration manipulation from the current network position to the optimal steady-state end point. RTO ensures the customer is supplied the required contractual ramping demand at all times, a contract requirement which is not currently always adhered to, and is able to robustly counteract process disturbances experienced by the network. The RTO strategy ensures the reconfiguration schedule of changing ASU loadings and compression occurs with optimal timing and within the safe limits. Currently, work is directed towards closed-loop implementation trials which requires an interface between the optimisation layers, the data historian and MPCs in order to automatically periodically send operating policy to plant, rather than being reliant on operator interface; however, process operators are still required to reconfigure the compression network until automated compression changes are programmed.

Furthermore, the robust implementation and operation of the RTO is dependent upon the weightings used in the RTO cost function. Overall, the resultant RTO objective function is a hybrid of economic optimisation, minimising power, liquid use and abortive power costs, and a control law, minimising the error between the site-wide set point targets and RTO outputs. As such, the cost function result is not representative of actual site-wide cost and a pragmatic approach is required to scale the control and economic penalty function weightings accordingly. In this work we have determined these via a pragmatic trial and error approach

after formulation of the RTO as an MILP. However, the determination of an optimal set of weightings could be considered an optimisation problem in its own right and we intend to further analyse the effect of these penalty weightings on the determination of an optimal plant reconfiguration. This could be achieved, for example, using additional representative sets of process operating (demand) data or the analysis of the problem through solution of a multi-objective optimisation problem and analysis of the Pareto optimal frontier, see Hawryluk et al. (2010). Likewise, current assumed safe ASU ramping limits may perhaps be limiting RTO performance leading to sub-optimal transitional solutions.

The current RTO strategy cannot, however, automatically plan over periods of lower power pricing to recover those stocks, as suggested in Adamson et al. (2017), by producing liquid at other times, but this can be achieved by developing a discrete time forward optimisation and scheduling method as suggested by Manenti et al. (2013) and Floudas and Lin (2005). For optimisation problems involving more decision variables and constraints than the permitted programmable number in the free Excel solver software version would need the license purchase for the commercial version or a different optimisation platform. Further, controller host computers do not have unrestricted access to the internet for security reasons and use of other optimisation platforms will require a guarantee against withdrawal for futureproofing.

Discrete time optimisation could deliver considerable further benefits (through the observation of future network changes before they occur and therefore prepare the network for change) across a future scheduling horizon including; reduction of power consumption during network transitions, minimisation of liquid back up consumption, reduction of LP gas spill and minimisation of machine wear due to starting and stopping compressors. Further benefits could include inclusion of ASU dynamics, development of more sophisticated modelling and optimisation architectures and modelling of uncertainty, as shown in Zhu et al. (2011). However, discrete time optimisation across a future horizon would require better than current forecasts of customer demands and power pricing, with uncertainty known to cause forecast inaccuracies, Huang and Biegler (2012). It is therefore an open question as to whether this would be beneficial in a practical application modelling the demand uncertainty may not lead to a robust real-time optimisation strategy. To this extent, it would therefore be difficult to determine optimal maintenance scheduling, suggested by Kopanos al. (2015), due to the day-ahead customer demand uncertainty, plus the random nature of machine trips and the costs of technician stand-by.

Finally, it should be noted that the proposed strategy is implemented in Excel (and interfaced through the plant historian), making the technology transferable to SMEs e.g. small scale biomass regeneration plants, cement factories etc. where investment in commercial RTO software may be prohibitive. It is envisaged that reconfiguration costs, such as man-hours required to recharge a cement vessel, can be modelled similarly as a RTO strategy.

Acknowledgments

The authors gratefully acknowledge the financial support of EPSRC grant EP/G037620/1 and BOC Gases through the Biopharmaceutical Bioprocessing Technology Centre at Newcastle University, UK.

References

Adamson, R., Hobbs, M., Silcock, A., Montague, G. (2015). "Real Time Optimisation of Industrial Gas Supply Networks." IFAC-PapersOnLine 48(8): 355-360.

Adamson, R., Hobbs, M., Silcock, A., Willis, M. J. (2017) “Steady-state optimisation of a multiple cryogenic air separation unit and compressor plant” Applied Energy 189 221-232

Baldea, M., Harjunkoski, I. (2014) “Integrated production scheduling and process control. A systematic review” Computers & Chemical Engineering 71 377-390

Cortinovis, A., Mercangoz, M., Zovadelli, M., Pareschi, D., De Marco, A., Bittanti, S. (2016) “Online performance tracking and load sharing optimization for parallel operation of gas compressors” Computers and Chemical Engineering 88 145-156

Engell, S. (2009). “Online optimizing control: The link between plant economics and process control” 10th Int. Symposium on Process Systems Engineering 79-86

European Commission (2015) “Horizon 2020 work programme 2016-2017 17. Cost cutting activities (focus areas)” 49-50

Floudas, C. A., Lin, X. (2005). “Mixed integer linear programming in process scheduling: modelling, algorithms, and applications” Annals of Operations Research 139 131-162

Hawryluk, A., Botros, K. K., Golshan, H., Huynh, B. (2010) “Multi-objective optimization of natural gas compression power train with genetic algorithms” 8th International Pipeline Conference (3) 421-435

Heidarinejad, M., Liu, J., Christofides, P. D. (2012) “Economic model predictive control of nonlinear process systems using Lyapunov techniques” AIChE Journal 58 (3) 855-870

Hovd (2007) “Improved target calculation for model predictive control” Modeling, Identification and Control 28(3) 81-86

Huang, R., Biegler, L. T. (2012) “Economic NMPC for energy intensive applications with electricity price prediction” 11th International Symposium on Process Systems Engineering (Computer Aided Chemical Engineering) 31 1612-1616.

Kopanos, G. M., Xenos, D. P., Cicciotti, M., Pistikopoulos, E. N., Thornhill, N. F. (2015). "Optimization of a network of compressors in parallel: Operational and maintenance planning – The air separation plant case." Applied Energy 146: 453-470.

Kurz, R., Winkelmann B. and Mokhatab S. (2010). "Efficiency and Operating Characteristics Of Centrifugal And Reciprocating Compressors." Pipeline and Gas Journal 237(10).

Li, T., Roba T., Bastid M. and Prabhu A.. (2011) "Real time optimization of air separation plants." Proceedings of ISA Automation Week 2011.

Lotero, I., Robab, T., Gopalakrishnana, A. (2017) “Supply risk limits for the integration of production scheduling and real-time optimization at air separation units” Foundations of Computer Aided Process Operations / Chemical Process Control Conference 2017

Love, J. (2007) “Process Automation Handbook: A Guide to Theory and Practice” Springer Science & Business Media Chapter B7 849-899

Manenti, F. and M. Rovaglio (2013). “Market-driven operational optimization of industrial gas supply chains” Computers & Chemical Engineering 56: 128-141.

Marchetti, A. G., Ferramosca, A., Gonzalez, A. H. (2014) “Steady-state target optimization designs for integrating real-time optimization and model predictive control” Journal of Process Control 24 129-145

Merkert, L., I. Harjunkoski, Isaksson, A., Saynevirta, S., Saarela, A., Sand, G. (2014). “Scheduling and energy – Industrial challenges and opportunities” Computers and Chemical Engineering 72: 183-198.

Pattison, R. C., Touretzky, C. R., Harjunkoski, I., Baldea, M. (2016) “Moving horizon closed-loop production scheduling using dynamic process models” American Institute of Chemical Engineers Journal 63(2) 639-651

Paparella F., Domínguez L., Cortinovis A., Mercangöz M., Pareschi D and Bittanti S. (2013) “Load sharing optimization of parallel compressors.” European control conference (ECC), July 17–19, 2013, Zürich, Switzerland.

Puranik, Y., Kilinç, M., Sahinidis, N. V., Li, T., Gopalakrishnan, A., Besancon, B., Roba, T., (2016) “Global optimization of an industrial gas network operation” American Institute of Chemical Engineers Journal 62(9) 3215-3224

Singh, R., Sen, M., Ieraperitou, M., Ramachandran, R. (2015) “Integrated moving horizon-based dynamic real-time optimization and hybrid MPC-PID control of a direct compaction continuous tablet manufacturing process” Journal of Pharmaceutical Innovation 10 233-253

Schmidt, W. P., Winegardner K. S., Dennehy, M., Castle-Smith, H. (2001). "Safe design and operation of a cryogenic air separation unit" Process Safety Progress 20(4): 269-279.

Tatjewski, P. (2010) “Supervisory predictive control and on-line set-point optimization” International Journal of Applied Mathematics and Computer Science 20(3) 483-495

Xenos D. P., Cicciotti M., Kopanos G. M., Bouaswaig A. E. F., Kahrs O., Martinez-Botas R. and Thornhill N. F. (2015). “Optimization of a network of compressors in parallel: Real Time Optimization (RTO) of compressors in chemical plants – An industrial case study” Applied Energy 114 51-63

Würth, L., Rawlings, J. B., Marquardt, W. (2009) “Economic Dynamic Real-Time Optimization and Nonlinear Model-Predictive Control on Infinite Horizons” IFAC Proceedings Volumes 42 (11) 219-224

Zhou, D., Zhou, K., Zhu, L., Zhao, J., Xu, Z., Shao, Z., Chen, X., (2017) “Optimal scheduling of multiple sets of air separation units with frequent load-change operation” Separation and Purification Technology 172 178-191

Zhu, Y., Legg, S., Laird, C. D. (2011) “Optimal operation of cryogenic air separation systems with demand uncertainty and contractual obligations” Chemical Engineering Science 66(5) 953-963